Aalborg Universitet

Communication Architecture Designs of Smart Inverters for Microgrids

Arbab Zavar, Babak

Publication date:
2022

Document Version
Publisher's PDF, also known as Version of record

Link to publication from Aalborg University

COMMUNICATION ARCHITECTURE DESIGNS OF SMART INVERTERS FOR MICROGRIDS

BY
BABAK ARBAB-ZAVAR

DISSERTATION SUBMITTED 2022

AALBORG UNIVERSITY
DENMARK

Communication Architecture Designs of Smart Inverters for Microgrids

Ph.D. Dissertation
Babak Arbab-Zavar

Dissertation submitted month 05, 2022

Abstract

The microgrid (MG) concept was established on the idea of localizing energy generation and consumption while utilizing as many renewable resources as possible. In this respect, the dependence on centralized generation running on conventional fossil fuels is minimized and extensive losses of large distribution systems can be avoided. In MG scenarios, since localizing is the key, machine-to-machine (M2M) communications are tended to be minimized. However, M2M communication frameworks are still required, and this PhD thesis is about investigating this problem and offering solutions that can fulfil the requirements and overcome existing issues from a new perspective. In this thesis that is derived from four journal papers (three published and one submitted), several issues related to the role of communication in MG management are addressed and discussed in detail.

At the first step, specifications of smart inverters were introduced and conceptualized. These power-electronics-based devices act as power interfaces between distributed generators (DGs), loads, and energy storage systems (ESSs) with the MG bus. Properly designed and implemented M2M communication architectures are one of the main requirements of smart inverters which were explained and justified in this step.

At the next part, a communication architecture was proposed that may successfully be employed into grid-connected (GC) MG systems to properly control the storage unit and minimise energy trades with the stiff grid at the point of common coupling (PCC). In this part, the communication network was fully developed from scratch by using micropython-enabled microcontrollers that are low power devices and can support the internet of things (IoT) ideology. Moreover, the message queuing telemetry transport (MQTT) application protocol was selected for messaging according to its lightweightness and publish/subscribe methodology, therefore the whole design was aiming to reduce energy expenditure and complexity. Alongside the communication framework design, the MG model formed on grid-feeding (GFD)

inverters was also designed and implemented on an experimental testbed, and results were provided to validate this integration.

The physical layer protocol of the aforesaid communication architecture was short-range (WiFi). This issue might cause limitations if the specific MG of interest contains geographically widespread units which motivated the next part of this thesis. Long-range protocols were studied and specifically low-power, wide area network (LPWAN) technologies were considered as a solution to the coverage problem. Among the various protocols and systems LoRaWAN was selected owing to its range, implementation simplicity, and possibility to construct private networks. In this accord, a LoRa enabled smart inverter model was prepared and experimentally evaluated. Such a smart inverter can connect widespread DGs, or ESS with each other or an MG central controller (MGCC) in an effective and dependable fashion.

In the next part of this thesis, the effects of transmission link-loss on MG optimum performance were explained and investigated. Knowing that depending on the MG architecture and the kind of power-converters used, the communication function on management and control paradigms differs, the identical MG structure of the earlier parts of the study was used here again for the sake of consistency. In this section, short-term load/generation forecasting methodologies based on deep learning (DL) techniques were performed on synthetically generated databases. These forecastings were used to assist the energy management system (EMS) to anticipate future time-step power setpoints for the storage unit. Consequently, the battery is loaded with supplementary information that can help to mitigate the detrimental repercussions of communication link-losses.

As final remarks and to provide a brief summary of the work, it may be said that in this PhD project the role of communication on AC-MG management was investigated from both communication science and control engineering viewpoints. This represents a non-trivial and challenging approach that require deep understandings of both areas of technology. Device-level models for control and messaging systems were developed, the integration methodology was presented, and different operational scenarios were evaluated and experimentally validated. The reason that both of the aforesaid points of view are included is the factor that can distinguish this research from similar studies.

Resumé

M icrogrid-konceptet (MG) blev etableret ud fra ideen om at lokalisere energiproduktion og -forbrug og samtidig udnytte så mange vedvarende ressourcer som muligt. I denne henseende minimeres afhængigheden af centraliseret produktion, der kører på konventionelle fossile brændstoffer, og omfattende tab af store distributions systemer kan undgås. I MG-scenarier, da lokalisering er nøglen, har maskine-til-maskine-kommunikation (M2M) tendens til at blive minimeret. M2M kommunikations rammer er dog stadig nødvendige, og denne ph.d.-afhandling handler om at undersøge dette problem og tilbyde løsninger, der kan opfylde kravene og overkomme eksisterende problemstillinger fra et nyt perspektiv. I denne afhandling, der er afledt af fire tidsskriftsartikler (tre offentliggjorte og en indsendt), behandles og diskuteres flere problemstillinger relateret til kommunikationens rolle i MG-ledelse i detaljer.

På det første trin blev specifikationer for smarte invertere introduceret og konceptualiseret. Disse strømelektronik baserede enheder fungerer som strømgrænseflader mellem distribuerede generatorer (DG'er), belastninger og energilagrings systemer (ESS'er) med MG-bussen. Korrekt designede og implementerede M2M-kommunikations arkitekturer er et af hovedkravene til smarte invertere, som blev forklaret og begrundet i dette trin.

I den næste del blev der foreslået en kommunikations arkitektur, der med succes kan anvendes i nettilsluttede (GC) MG-systemer for korrekt at kontrollere lagerenheden og minimere energihandler med det stive net ved punktet for fælles kobling (PCC). I denne del blev kommunikationsnetværket fuldt udviklet fra bunden ved at bruge mikropython-aktiverede mikrocontrollere, der er laveffektenheder og kan understøtte internet of things (IoT) ideologi. Desuden blev MQTT-applikations protokollen for beskedkøtelemetritransport valgt til meddelelser i henhold til dens letvægt og publicerings /abonnement metodologi, og derfor sigtede hele designet på at reducere energiforbrug og kompleksitet. Ved siden af kommunikationsramme

designet blev MG-modellen dannet på grid-feeding (GFD) invertere også designet og implementeret på en eksperimentel testbed, og resultater blev leveret til at validere denne integration.

Den fysiske lagprotokol for den førnævnte kommunikations arkitektur var kort rækkevidde (WiFi). Dette problem kan forårsage begrænsninger, hvis den specifikke MG af interesse indeholder geografisk udbredte enheder, som motiverede den næste del af denne afhandling. Langrækkende protokoller blev undersøgt, og specifikt low-power, wide area network (LPWAN) teknologier blev betragtet som en løsning på dækningsproblemet. Blandt de forskellige protokoller og systemer blev LoRaWAN udvalgt på grund af dets rækkevidde, implementerings simpelhed og muligheden for at konstruere private netværk. I denne aftale blev en LoRa-aktiveret smart invertermodel forberedt og eksperimentelt evalueret. Sådan en smart inverter kan forbinde udbredte DG'er eller ESS med hinanden eller en MG central controller (MGCC) på en effektiv og pålidelig måde.

I den næste del af denne afhandling blev virkningerne af transmissionsforbindelsestab på MG-optimal ydeevne forklaret og undersøgt. Ved at vide, at afhængigt af MG-arkitekturen og typen af anvendte strømkonvertere, er kommunikations funktionen på styrings- og kontrolparadigmer forskellig, den identiske MG-struktur i de tidligere dele af undersøgelsen blev brugt her igen for sammenhængens skyld. I dette afsnit blev kortsigtede belastnings /generations prognosemetoder baseret på deep learning (DL)-teknikker udført på syntetisk genererede databaser. Disse prognoser blev brugt til at hjælpe energistyringssystemet (EMS) til at forudse fremtidige tidstrins-effekt indstillings punkter for lagerenheden. Følgelig er batteriet fyldt med supplerende information, der kan hjælpe med at afbøde de skadelige følger af tab af kommunikations forbindelser.

Som afsluttende bemærkning og for at give en kort opsummering af arbejdet kan det siges, at i dette Ph.D. projekt blev kommunikationens rolle på AC-MG-ledelse undersøgt ud fra både kommunikationsvidenskab og kontrolteknik synspunkter. Dette repræsenterer en ikke-triviel og udfordrende tilgang, der kræver dyb forståelse af begge teknologiområder. Modeller på enhedsniveau for kontrol- og meddelelsessystemer blev udviklet, integrationsmetodikken blev præsenteret, og forskellige operationelle scenarier blev evalueret og eksperimentelt valideret. Grunden til, at begge de førnævnte synspunkter er medtaget, er den faktor, der kan adskille denne forskning fra lignende undersøgelser.

Preface

The work presented in this thesis is a summary of the outcome from the Ph.D. project "Energy Management Systems based on IoT/ Energy Internet for Smart Homes", which was conducted at the Department of Energy Technology, Aalborg University, Denmark.

This work was performed under the supervision of Prof. Josep M. Guerrero and co-supervision of Prof. Juan C. Vasquez and Dr. Emilio J. Palacios-Garcia at the Department of Energy Technology, Aalborg University. The period of this study was from October 2018 to March 2022. During this period a study abroad was conducted from March 2021 until October 2021 at the University of Southampton, Mechatronics Research Group, Under the supervision of Prof. Suleiman Sharkh. Nevertheless, due to the travel and stay restrictions this visit was not physical and the regular biweekly meetings with Prof. Suleiman Sharkh were online using the MS Teams platform.

I am eternally grateful to all my supervisors for the endless time and efforts they spent during this study period. This would not be possible without their top-class and very considerate supervision. I would like to thank all the academic and official staff of AAU-Energy, Aalborg University for providing support and assistance whenever required. In addition, heartfelt appreciation to all my friends and colleagues in CROM Research group & AAU-Energy, Aalborg University that made this difficult task feel easy.

Finally, I would like to deeply thank my family for their kindness, endless support, and unconditional love that led me to find the path throughout my entire life. There are no words to express my level of gratitude in this regard.

Babak Arbab-Zavar
Aalborg University, May 30, 2022

Preface

Contents

II Papers 81

List of Figures

List of Tables

Part I

Report

Chapter 1

Introduction

N owadays, with the expansion of sustainable energy penetration into the energy networks the concept of distributed generation has become more popular. The idea is to convert energy consumers into active prosumers, which consume, produce, and occasionally export energy at the same station [2]. One of the benefits of distributed generation, apart from the utilization of renewable energies, is to decrease the size of equipment and structures at the transmission and distribution level, therefore, lowering the capital implementation costs. To put it another way, the grid will be downsized contributing to lowering transmission losses.

The microgrid (MG) concept is centred on the ideology of scattered generation [3]. A grid consisting of a number of generators and loads that are electrically connected and fully controllable, which has the capability to synchronize and interact with other grids is called an MG [4]. The term micro, which refers to the scale and size of this specified network, is open to interpretation and that resulted to the emergence of other terms such as nano-grids or pico-grids [5]. Despite the scale, the presence of these weak grids becomes relevant due to their capability of operating in isolation together with grid-connected (GC).

As previously stated, MGs may work in either isolated or GC mode. In the event of the former, the main considerations are proper power sharing to avoid harmful current circulations, power quality, and also voltage magnitude and frequency synchronization between the internal MG units. When a stiff grid is present and interactions are unavoidable, other aspects like frequency synchronization, unintended islanding detection, and active/reactive power exchange management at the point of common coupling (PCC) become crucial to investigate. One situation which leads to a favorable interaction with another grid is when, in respect of energy production and expen-

diture, there is not an internal balance within the MG. However, in a number of instances when the production dominates the consumption, it does not force an exchange with other grids since the MG structure normally consists of energy storage systems (ESSs). As another possibility, the generation side can be shut down or set to produce lower power than it is actually able to produce.

MGs came into existence owing to the deployment of power converters. These converters are used to interface each distributed generator (DG) with the bus and their role is not just to convert between nonidentical kinds of power signals but also to make the feeders controllable. Different control algorithms can be administered by manipulating the converter's gate firing signals. According to their configuration and control scheme converters are categorized into grid-forming (GFM), grid-feeding (GFD), and grid-supporting. Voltage source inverters (VSI) as well as current source inverters (CSI) belong to the grid-supporting category and their structures are slightly different [6]. CSIs are normally used for renewable sources and require a voltage reference to operate. Therefore, they may be utilised in MG structures that are coupled with a stiff grid since the setpoints are appointed by that grid, or in isolated mode if another voltage source is available. On the contrary, VSIs have the capability to regulate the voltage magnitude and frequency.

1   Communication and MG control

In compliance with the further development of MG control strategies, they became less communication-dependent and more reliant on local sensory readings. Hierarchical control that is founded on droop methodology is a well-established criterion in control for GFM based structures. This multi-layer control scheme was developed and proposed considering the goal of making the control as autonomous and distributed as possible. It consists of three different stages. The bottom level, which includes inner loops and droop controllers is in charge of ensuring stability and is communication-free. As a repercussion of implementing droop methods, deviations from the nominal values of voltage magnitude and frequency will occur. The objective of the secondary control is to recompense these deviations, restoring the reference values. From this level upwards, communication is required and accessibility to local measurements on each converter is not sufficient anymore. The next level, which is called the tertiary level, regulates the power flow from or toward the MG. At the tertiary level, the error between the power flow magnitudes and their references, calculated by the energy management system (EMS), is minimized. Both the secondary and tertiary levels require communication since the control parameters are not only local measurements [7–10]. Figure 1.1 illustrates the hierarchical schema for MG con-

Fig. 1.1: MG control hierarchy.

trol where the integration of the messaging links into the control architecture can be clearly seen [11].

The technical aspects of the abovementioned communication links are normally overlooked by MG-related research publications. In fact, in the simulation part of most of these studies usually, a time delay block is exploited to imitate the network links and, in our opinion, this is far from ideal. To rephrase it, if an MG model aims to provide realistic results it should contain comprehensively modeled communication structures. The importance of this aspect emerges because of the possibility and probability of various types of faults, occurring inside a multi-layer messaging framework. For example, complications such as packet losses, degradations in the quality of the signal, packet collisions, duplications, and ultimately complete failures. These sorts of challenges are considered more in the studies related to smart grids (SGs). The best examples of MG studies with communication considerations are researches on secondary controllers, multi-MG investigations, and cyber-attack studies. Other MG researches are mostly not related to communication.

As briefly explained before, communication dependency of the hierarchical scheme starts from the secondary level. This level contributes to the overall control of an AC-MG system by fulfilling three objectives:

- Compensate for frequency deviations due to load changes as a consequence of the frequency - active power droop controller.

5

- Reset the voltage magnitude to its reference values.

- Contribute to proper reactive power-sharing. Since exists a trade-off between voltage adjustment and reactive power-sharing at the bottom level and accurate power-sharing paradigm can not be achieved without secondary control. This problem arises as a consequence of the difference in the output impedance of each inverter with the other corresponding units so the voltage magnitudes are different which is opposite to the frequency. Therefore, even in the case of parallel-connected inverters with the same characteristics, reactive power can not be shared proportionally only by the voltage-reactive power droop control [12,13].

Secondary controllers, which represent the top level of the hierarchy in isolated mode, are categorized into centralized (CSC) and decentralized (DSC) methods, figure 1.2. CSC method compares real-time $V \& f$ measurements of the bus with their reference values (offered by the tertiary level) and transmits their deviations to the local controllers of each DG via a communication link. This approach contains an obvious flaw which is the danger of a single point failure occurrence on the bus $V \& f$ measurements, or the messaging system. Besides, the communication structure may become too complex and the capital implementation and operating costs can be high. [12–18].

Due to the inefficiencies accompanied by the conventional CSCs, DSC methods have been designed. DSC algorithms are based on communication among DGs and perform control actions locally rather than following a central unit. The idea is to limit the communication to only the neighbouring devices and, using averaging or consensus methods, agree on certain values which emulate the entire system characteristics [13,14,17,19,20].

To put it another way, by using DSC methods, the communication infrastructure scales down, the complexity decreases, and the vulnerability to single-point errors is eliminated. Figure 1.2a illustrates the centralized method and figure 1.2b represents the decentralized concept for secondary control. In both figures, the messages which are transmitted through the communication structure are highlighted by using red color. These figures are conceptual and do not provide a quantitative measure for the network scale and amount of messages passing through them. However, as it is shown in figure 1.2a the secondary controller operates on the voltage magnitude and frequency readings from the main bus which means there is a possible vulnerability to a single point failure present.

It is noteworthy that the discussion provided above is in accordance with MG architectures based on GFM converters. If GFD inverters are utilized the secondary control plays a rather different role. However, the actuality that this level is depending on machine-to-machine (M2M) communication links remains intact. Figure 1.3 illustrates and explains the aforementioned difference.
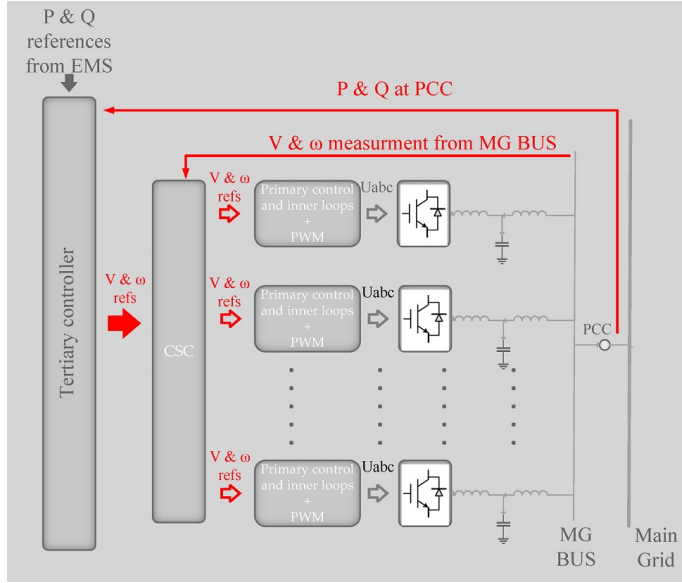
(a) CSC
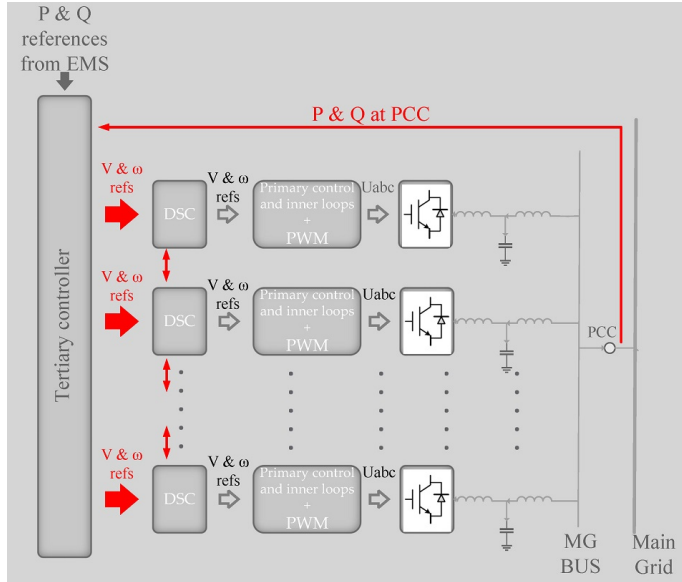
(b) DSC

Fig. 1.2: Centralized and decentralized secondary controllers.

Having provided a brief introduction on the communication role in MG
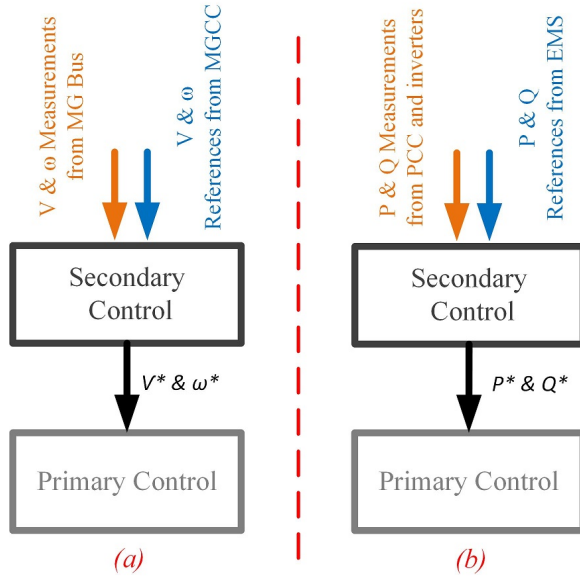
Fig. 1.3: Different role of secondary control, (a) GFM inverters, (b) GFD inverters.

management, here a number of major real-world implementation and operation challenges are listed as follows:

- Availability: In some real-world scenarios an accessible and proper communication network is not always present. For instance, in rural applications where convectional network links are not available. This means the link needs to be created and designed initially and should not be assumed as existing.

- Heterogeneity: Different devices in a communication structure may be from various types and manufacturers. Therefore, even in up-and-running networks, if the machines are not compatible with the messaging protocols and standards, meaningful transmission is not possible. To put it another way, if this issue is not properly addressed even a perfect communication infrastructure will become useless since the devices either can not receive and send or can not understand what they are receiving.

- Packet losses and packet duplication: This problem may easily happen when the network traffic is high or unstable.

- Signal degradation and noises: This problem mainly concerns power line communication protocol (PLC) because of the electrical interactions
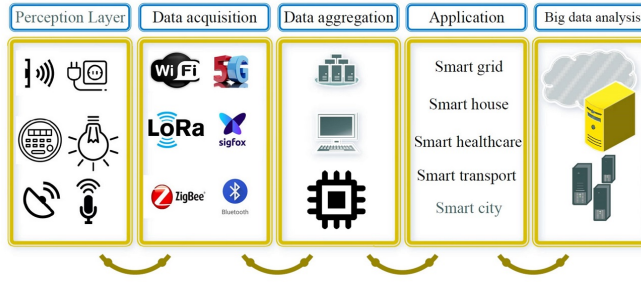
Fig. 1.4: Five layer IoT architecture.

of several devices attached to the same wire. More recently wireless networks have also faced such disturbances.

2 Internet of Things (IoT) and Cyber Physical Systems (CPS)

IoT has been a hot topic since the introduction of the concept two decades ago. One global definition can not be found for IoT since different people interpret the concept from their own perspective and the application of interest. As a popular definition, IoT is a platform for some physical and smart devices to coordinate decisions and perform their duties with minimal or no user intervention by equipping them with state-of-the-art digital communication capabilities [21–25]. Paying attention to IoT definition, clear similarities may be recognized with how the SG idea is interpreted. As a matter of fact, SGs are one of many IoT applications similar to smart-healthcare, smart-education, smart-transportation and many more [26, 27]. Since MGs also belong to the classification of SGs, investigating the IoT concept is necessary to be incorporated in this work. Figure 1.4 illustrates a five-layer IoT infrastructure and as it is shown, communication protocols play a crucial role in IoT systems.

It is worth noting that, there is a common mistake that refers to IoT as a technology which is not true by any means. IoT is a framework that consists of physical devices, communication networks, sensing identification, and processing algorithms.

From a slightly different perspective, the concept of CPS has been introduced. CPS is a number of physical units linked through a cyber environment, which translates to the presence of digital communication channels and state-of-the-art computational methods [28]. A clear distinction between the two concepts of IoT and CPS can not be established, however, in some

literature, IoT is defined as the interconnection feature between the communication layers of some numbers of CPSs [29]. In these studies, IoT is treated as a global-scale network of physical elements interconnected through the internet, providing pervasiveness and ubiquitous features to achieve effective interoperability [21–23].

Regardless of how complicated or how simple these concepts (IoT and CPS) are defined, what is important for this study is MGs can be conceptualized as an example for either of them. Furthermore, the foundation of these systems is M2M communication technologies. To express differently, the fact that MG systems, no matter if they are considered as IoT structures or CPSs, contain a lot of communication links between smart devices so they are needed to be thoroughly investigated from this viewpoint.

3 M2M communication

First of all, it is imperative to understand the dissimilarities between M2M and human-to-human (H2H) transmission networks. In the event of H2H communication, for instance, a video call, the requirements are large data rates for a limited number of users. Contrastingly, in M2M communications, the structure may consist of an extensive number of smart devices that sporadically transmit small packets. Therefore, the communication structure should be specifically designed to fulfill the requirements of the application [30]. Briefly, the predominant M2M communication characteristics can be listed as:

 i low packet-loss tolerance.

 ii Strict deadlines for delays.

 iii Robustness and resiliency in connection with possible damages.

There are also other required features such as wide coverage, higher battery life, and supporting an overwhelming quantity of devices especially when large-scale networks are been considered [31].

Following the methodology of the open system interconnection (OSI) standard communication model, a seven-layer stack should be designed for a proper communication structure. In this procedure, the protocol selection for the first (physical or PHY) and the last (application or messaging) layers gain more interest. Generally, the PHY protocol selection and implementation are strongly related to the topological characteristics of a specific grid. Contrastingly, the messaging protocols should be suitable with the processing capacity of the transceivers that are normally low, by design, in smart systems to save energy expenditure and capital cost. Some well-known application protocols suitable for M2M links are HTTP, MQTT, CoAP, and AMQP [11,32,33].
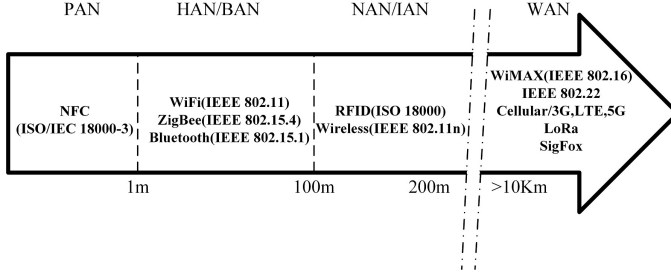
Fig. 1.5: Different wireless protocols classified in respect of coverage.

Each one of these messaging-level protocols has its own values as well as disadvantageous, so the selection of a fitting protocol relies upon the application nature and requirements. Between the two forenamed layers, there are five other layers that each have an important duty in the message encapsulation (or decapsulation) process by adding (or removing) headers to (from) the frame. Among them, we find the transport and network layers that host some widely-recognised protocols like transmission control protocol (TCP) and internet protocol (IP). Therefore, when designing a messaging network the whole stack should be considered, otherwise, physical and application level protocols cannot work in harmony to form a functioning communication structure.

One of the key factors for preferring and choosing a PHY protocol over the other available ones is the physical distance betwixt the elements of a system. The other characteristics that the selected transmission technology must contain to be suitable for these applications are low energy consumption, safe, resilience, and low implementation and operational cost. For example, in home automation IEEE 802.15.4 - 2.4 GHz may be an appropriate candidate. Contrastingly, if a personal area network (PAN) is in consideration, a lower power technology like near field communication (NFC) may be a better choice since the range required is very small [34]. Figure 1.5 illustrates some well-known wireless technologies and their corresponding nominal ranges [35–41].

To further explain the complexities of protocol selection an example is given. Let's consider the possibility to integrate MQTT messaging protocol into an already functioning ZigBee network. The rationalization for such an integration is to provide the likelihood of connecting normal IP devices (Android or Windows devices) to a home-automation system for better screening and monitoring. It is worth noting that ZigBee represents a whole communication stack while the IEEE 802.15.4 standard protocol represents its PHY and medium access layers (MAC). Contrastingly, the upper layers are specific to the ZigBee proprietary standard. As a design consequence, MQTT is

11

dictated to operate on top of a TCP/IP stack and determined by the length of its payload requires a certain data-rate constraint in the PHY protocol. At first glance, it seems that these two cannot be used together according to the incompatibility of different layer protocols. However, another version of MQTT named MQTT-SN has been developed to address this problem. This modified version of MQTT along with becoming even more lightweight and suitable for SG applications, is now compatible to work on top of ZigBee because of the reduction on the length of the frames so they may be handled by the bandwidth of IEEE 805.15.4 - 2.4 GHz [42, 43].

The ZigBee network is already globally used and is appropriate for home automation and other short-range applications. However, If the communications nodes are separated by large distances, on a scale of several kilometers, other PHY technologies are necessary to be considered. For example, LoRa is a low cost, low power, secure, and easy to exploit technology that provides extended coverage, therefore, it is a decent choice for very large-scale SG structures. It is worth noting, as opposed to ZigBee, LoRa just refers to the PHY layer and LoRaWAN defines both the MAC protocol and the system architecture. This architecture consists of three class of components [44–46]:

i End devices such as sensors, actuators, or smart devices.

ii Gateways, which convey the transmissions sent from the end–devices to a communication network server through some backhaul communication link (WiFi, Cellular, Ethernet, or other available technologies).

iii The Network server that is in charge of decoding the packets and creating response packets which are scheduled to be transmitted to the end devices.

Same as ZigBee network, it is also thinkable to use MQTT messaging protocol over a LoRaWAN network to benefit from the lightweight and easy-to-implement features of MQTT and the long-range feature of LoRa simultaneously. The system architecture consists of LoRa, as the physical channelling solution to connect the dispersed communication nodes to the gateways. These gateways first convert the LoRa frame payload to MQTT message format and after that transfer the packets to MQTT brokers as network servers. Other smart devices can be joined with the broker by other means of communication and subscribe to the messages which they are interested [44, 47].

4 MG communication layers

In the preceding subsections, the duty of messaging links on MG management was explained and different M2M communication protocols that may be utilised for such smart applications for sending and receiving messages

have been explained. However, the duty of communication in MG architectures is more complicated and contains several levels that are explained in this part and outlined in figure 1.6.

DAN	**Device Level** (Converters, V/I sensors, Data Loggers, Data Acquisition, …)	Low-Range High-Speed Ultra Reliability	• Can Bus • Modbus • Interbus • Profibus • Ethernet
SHAN	**Smart Home Level** (Smart Appliances, Control, Monitoring, Processing, …)	Heterogeneity Scalability Mobility	• ZigBee • WiFi • Zwave • Bluetooth • 6LoWPAN
MAN	**Microgrid Level** (DGs, ESSs, EV Charging, …)	Long-Range Independent Security	• LoRaWAN • SigFox • Dash7 • Ingenu • NB-IoT
MMAN	**Multi Microgrid Level** (Energy Internet)	Ultra Long-Range Terrain Affected Standardization	4G 5G Direct to satellite LPWAN

Fig. 1.6: MG communication layers, characteristics and protocol examples.

Device Level

This stage includes the internal communication between the power-electronics interfaces and their respective measurement devices. Local *V & I* readings can be acquired and used by control loops of the converters through the transmission channels of this layer. Nevertheless, their protocols have not been vastly investigated in energy-related researches since the function of messaging links does not directly contribute to power balance and exchanges between different DGs, loads, or ESS units at this level. Unlike the other communication levels of this architecture, this level, which is additionally the base level does not include wireless solutions. To rephrase it, the device level network is more of an industrial-grade communication system rather than being an IoT type platform and they are designed based on Fieldbus technologies [48]. The requirements and features of the device-level network are as listed:

- Real-time (RT) transactions are required since a delayed message can render the system unstable. The allowable latencies are not more than a few milliseconds [49]. Hence, wireless systems, especially the ones that are using TCP can not be considered for this level due to large latency measures [50]. It is worth noting that no communication can literally take place in real-time and there are always some latencies present,

which are in regard to the different stages of message encapsulation and transmission. To rephrase it, RT communication is a relative term.

- High measures of reliability, in the matter of decent deterministic behaviour, are expected which limits the relativity of wireless protocols for device-level. This is because of the likelihood of performance degradation in wireless systems as a consequence of signal interferences, noise problems, or other design-oriented issues [51]. Furthermore, an immune and unbreachable network is essential to ensure the crucial measurements can not be manipulated externally. Wireless is particularly vulnerable because of its broadcast operation nature so may not provide a safe enough link as demanded for this level.

Fieldbus technologies that aim to utilize proper MAC protocols to assure the aforementioned characteristics are appropriate candidates for this level of messaging structure. That is to say, these MAC protocols guarantee a collision-free medium and also prioritize the commands that are enforced to be relayed with higher latency restrictions [52]. The most popular Fieldbus technologies are, Modbus, Can Bus, Profibus, and Interbus. Further information on Fieldbus protocols and their characteristics may be obtained from another research paper, [53].

Smart-Home Level

Since smart-home is both a control-and-monitoring station and a residential building, this level of communication fulfils two distinctive roles simultaneously:

- Creating bidirectional links between power interfaces with central control processing units such as an EMS or an MG central controller (MGCC).

- Providing user monitoring and manipulation possibilities through human-machine interface (HMI) platforms.

The messaging frameworks of this level should be capable of supporting heterogeneity of devices, along with being scalable since adding new devices or removing old ones is an occasional phenomenon in residential applications. Besides, since here human interactions are important, mobility is another deciding factor since it provides a decent level of convenience for the users while reducing unnecessary wirings. Considering these characteristics, wireless technologies gain more relevance for this level and IoT-based networks may be productively utilized [21].

The most well-known messaging technology for smart appliances in smart homes is ZigBee thanks to its low-energy and cost-effectiveness characteristics [54, 55]. However, as previously mentioned, in smart-homes user inter-
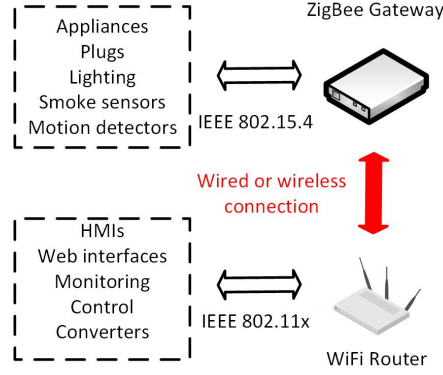
Fig. 1.7: Smart-home example network.

faces are also part of the communication network and because of the low-throughput characteristic of ZigBee or other proprietary protocols, they are not applicable for this side of the connectivity. To rephrase it, the wireless architecture for smart homes should include a low-power local area network (LPLAN) and a high-throughput LAN such as WiFi for best performance, figure 1.7. Several other protocols exist that may be selected for these sorts of applications, among them Bluetooth, Zwave, and 6LoWPAN are more popular [56].

MG Level

The main characteristics differences of MG level with the smart home level are:

- Longer range protocols are required since the DGs, ESSs, and other devices can be spread in a wider area where short-range technologies like ZigBee or WiFi are not capable of effectively covering.

- Since HMIs are not present and all the links in this level are of D2D type, high-throughput links are not necessary.

Low power wide area network (LPWAN) technologies, due to their long-range and low energy consumption may be very suitable candidates for the MG level [57]. Among them, LoRaWAN offers the practicability of creating private networks while using unlicensed frequency bands. Network privatizing can greatly contribute to a more secure environment that can prevent various types of unauthorized interferences [44,58,59]. There are other available LPWAN protocols that a number of more well-known ones are summarized in table 2.1.

Multi-MG Level

Unlike the MG level that localization and privacy are favorable, at this layer using standard and globally accessible protocols are more sensible. This is because, here, information is shared between various and different power systems that probably are not owned and operated by the same individuals/corporations and therefore may not support certain specific propitiatory communication protocols.

At this level, the required coverage is on the scale of several kilometers or much more which renders even LPWAN technologies useless for effective messaging. In addition, rough terrain may also harmfully affect the link quality especially when it is designed on line-of-sight dependency.

Because of these reasons, using cellular networks such as 4G and 5G may be contemplated as a perfect option for the multi-MG level. In the case of low network coverage phenomenon (that can happen in remote and underdeveloped regions) satellite-based messaging architectures and even direct-to-satellite LPWAN technologies may be considered as feasible solutions [60].

Chapter 2

Smart Inverters

As previously stated, in MG systems power-converters are used to interface each DG or ESS with the main bus. In compliance with the technological progress in this field, these converters are now able to effectively operate with less human intervention which defines the concept of *Smart Inverters* [10].

A key issue in the conceptualization of smart inverters is the role of M2M communication, as it is tended to be minimised to achieve more security considerations and autonomous operation but should be available to provide other smartness features. To rephrase it, proper communication architectures should be designed and implemented while modifying the control algorithms in a way that they are less communication-dependant. Based on this argument, an effective design and modelling of smart inverters require a deep understanding of both communication and control systems engineering and since multiple trade-offs are to be considered it may not be regarded as a simple and trivial matter.

In a manner of speaking, this PhD project is about the integration of different wireless communication architectures into smart inverters' control structures so providing a detailed explanation of these sorts of devices is necessary at this chapter.

1   Smartness indicators of smart inverters

The various indicators that define smartness characteristics for smart inverters are comprehensively discussed in [10,61]. Founded on the conceptualizations of these studies the indicators are demonstrated in figure 2.1 and are briefly explained in the following way:
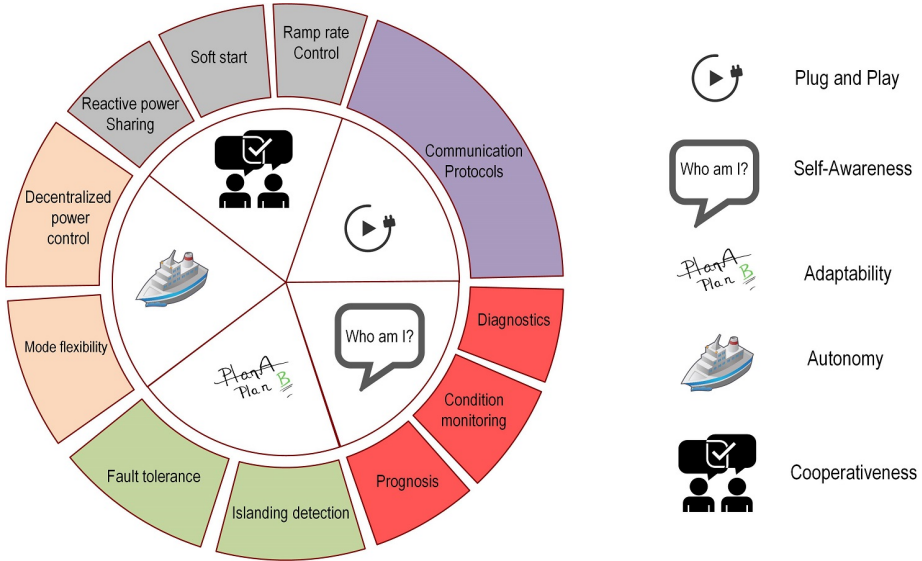
Fig. 2.1: Different indicators that may define smartness for smart inverters.

Plug and Play

This is a very important characteristic of any device that is going to participate in a smart system. It basically means, the device of interest (in this situation an inverter) may be blended into an already operating platform without the requirement of serious modifications on either the device or the platform sides. This is only possible if the device can *talk* to other devices and also *understand* their messages. To put it another way, the device must have the capability of comprehending the communication protocols that are implemented on the specific smart platform of interest. It is worth noting that various standard messaging M2M protocols are used to connect smart devices in smart platforms [10]. Therefore, a smart inverter should be designed in a way to be compatible with multiple communication protocols.

Self-Awareness

This characteristic of smart inverters is not related to communication architectures and systems. The definition of self-awareness, as it can be comprehended from the title is the ability of the device to monitor its health status, conduct diagnostics in the event of a failure occurrence, and also perform prognosis for possible future problems [10, 62, 63].

The aforementioned self-awareness features of smart inverters can be either achieved by implementing proper protection hardware devices such as

relays or by utilizing software-based solutions to detect more difficult to find and locate open-circuit failures [64].

As previously noted, since this smartness indicator is not related to M2M messaging structures and their integration into control structures, it will not be further investigated in this PhD thesis.

Adaptability

In some applications, the presence of a stable and reliant grid is so crucial that the smart inverters have to remain operational even in faulty situations. Nonetheless, if unintentional islanding happens, in line with the stiff grid failure, the smart inverter must be capable to instinctively detect the phenomenon and perform proper precautionary measures to prevent harmful situations. Fault tolerance and unintended islanding detection, define another smartness indicator for smart inverters called adaptability.

- Fault tolerance: This characteristic is achieved by two methods. In the first method, the inverter structure is equipped with redundant hardware which can be in respect of extra switches, legs, modules, or even whole devices. These are utilised when a faulty unit is detected and put out of service. The second method is founded on manipulating the modulation to balance out a fault and achieve the desired grid characteristics with the new configuration, while bypassing problematic units [65,66].

- Unintended islanding detection: This procedure can be conducted either remotely or locally. The former method requires communication and is founded on monitoring the grid parameters at the consumer's end. Local methods which are performed on the smart inverter side are further subcategorized to active and passive methods where supplementary descriptions may be obtained from, [10,67].

Autonomy

Although communication links are necessary and play a key role in MG management & control, it is favorable to minimise them so that extra costs and complexities in the entire architecture may be omitted. That is to say, smart inverters must be capable of operating as autonomously as possible.

One way to achieve autonomy is to implement a communication-free primary level in their control structures based on droop methodology [10,68,69]. In such manner, parallel power-sharing may be acquired without benefiting from central controllers and communication links.

Furthermore, the smart inverters must be capable of switching their modes of operation without operator intervention whenever necessary. This is a re-

quirement when the MG switches from GC to islanded or the other way around so that some inverters are required to change their operational modes to adapt to the new conditions. In addition these mode changes should occur in a smooth manner to not disturb the consumers and cause harmful effects [10,70,71].

Cooperativeness

Another important characteristic that is worth mentioning is cooperativeness with other units in an MG infrastructure. This includes features such as ramp rate control, soft start, and many more [10,72].

2   Communication protocols for smart inverters

So far in this chapter, the smartness indicators have been briefly introduced and investigated. Based on these discussions, communication plays a vital role in this regard, therefore, common protocols and technologies that may be incorporated into smart inverter's control algorithms are explained in this part.

Table 2.1: Technical characteristics of smart inverter communication protocols.

Protocol	Technology	Range	Rate	Remarks
WiFi	Wireless	100 m	MAX 54 Mbps	Limited coverage-High throughput
ZigBee	Wireless-LPLAN	100 m	MAX 250 kbps	Low throughput-Low power
Bluetooth	Wireless	15 m	1-2 Mbps	Very short range-Ultra reliable
UWB	Wireless	10 m	110 Mbps	Very short range-High throughput
GSM	Wireless-Cellular	10 km	MAX 14.4 kbps	Low data rate
GPRS	Wireless-Cellular	10 km	MAX 170 kbps	Low data rate
3G	Wireless-Cellular	10 km	MAX 2 Mbps	High operational costs
WIMAX	Wireless-Cellular	50 km	MAX 75 Mbps	Elusive-High coverage/throughput
SigFox	Wireless-LPWAN	10-40 km	100-600 bps	Limited daily messages-Long range
LoRaWAN	Wireless-LPWAN	1-15 km	MAX 50 kbps	Private network allowed-Long range
Dash7	Wireless-LPWAN	1-2 km	MAX 150 kbps	Medium range
Ingenu	Wireless-LPWAN	15 km	156-624 kbps	Higher power consumption
PLC-NB	Wired	150 km	10-500 kbps	Signal degradation-Low throughput
PLC-BB	Wired	1.5 km	10-200 Mbps	Signal interference-Short range
PON	Fiber optics	10-60 km	100-2500 Mbps	Not cost effective
AON	Fiber optics	10 km	100 Mbps	Upgrade difficulties

A smart inverter can communicate by either wired or wireless technologies with other MG elements. In addition, exist a various number of protocols and architectures for each of the forenamed frameworks. Generally speaking,

there is not a definite rule of thumb about what protocol must be chosen for a smart inverter and it largely relies on the purpose the device is going to be used for.

In table 2.1 some well-known communication protocols are presented [10, 44], and as it may be comprehended each protocol contains some benefits accompanied by a few drawbacks. In the next chapters of this PhD thesis, some of these protocols are utilised to be implemented into smart inverters' operational paradigms.

3

Communication framework for AC-MG energy management

Following the previous argumentations and explanations in respect of communication networks and MG architectures, plus the smartness conceptualization for inverters, in this chapter, a proposed messaging infrastructure for GC-AC-MG is unveiled. In this suggested architecture, both communication and control algorithms are included, and the system behaviour is experimentally evaluated in normal and various faulty scenarios.

Problem definition: As explained before, to effectively control an MG, M2M communication links are required. If the system is GC the inverters' operation mode is mostly GFD since the voltage magnitude and frequency of the bus are fixed while synchronising with the stiff grid, so GFM types are not compulsory. In addition, in these kinds of MG configurations, an ESS is normally included that contributes to balancing energy internally and minimising power trading at the PCC. This ESS that is equipped with a smart inverter requires to receive proper power references at each time step in line with the instantaneous production and depletion values.

Because of the absence of extensive computational resources in such inverters, the aforementioned power references should be calculated by an off-site EMS. Therefore, a transmission network is indispensable to convey the output power measurements of each unit along with the ESS state of charge (SoC) towards the EMS and return calculated power setpoints.

It is worth noting, the MG model is created to simulate a homelike MG

scenario (Smart-home) and the goal is to minimise PCC power traffic as much as possible.

1 Communication architecture development

Designing a communication structure is not just about selecting a PHY protocol such as LoRa or WiFi since a transmission system is a multilayer architecture respecting the OSI template. This model contains several layers and either of them supports a number of standard protocols. It can be simplified to the IoT stack with fewer layers and more fitting for the application of concern in this thesis, figure 3.1. As it may be noted, several protocols are available for each layer and these are just examples of many more [11].

So, what is the paradigm of selecting proper protocols and designing the whole stack? In this point we are aiming to address this question.

1.1 Protocol selection

To design an effective transmission system for a smart application, such as an AC-MG some points should be carefully considered.
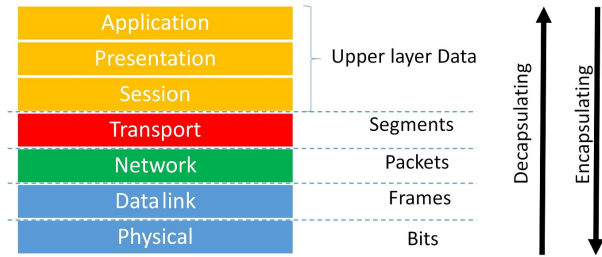

(a) OSI
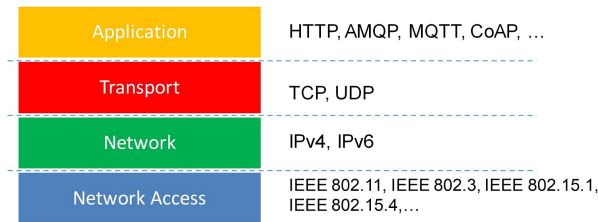
(b) IoT

Fig. 3.1: OSI and IoT stacks.

- The actual dimension of the framework is a deciding factor for the physical or network access protocol since all of them cannot provide the requested coverage.

- The data rate requirements are another important factor since there is a tradeoff between throughput and power consumption. For example, paying attention to the first row in table 2.1 it may be acknowledged that the data rate of ZigBee is much less than WiFi but it is a low-power protocol and therefore more appropriate for M2M application where the units may be battery-powered.

- The processing capacity of the transceivers are an important issue while choosing the messaging (top) layer protocol since some of them are designed to be lightweight (in respect of header sizes) and less complex. For example, MQTT header structuring and publish/subscribe methodology is much simpler than HTTP (which is based upon request/response) so it is a better candidate for M2M scenarios with limited computational and bandwidth (BW) resources [11].

In a few words, at the process of designing a communication architecture the proper methodology is to select an *"application level"* protocol by considering the required messaging characteristics, type of end-users and also computational limitations and then chose a *"network access level"* protocol by paying attention to the necessary coverage, due to the topological aspects of the infrastructure, and the desired throughput. Security considerations should also be considered while selecting these protocols and designing the complete communication stack.

The intermediate layers are normally selected in a way that the top *"application layer"* and bottom *"network access layer"* protocols can interoperate effectively. By way of explanation, although these layers have their specific roles and are crucial in the transmission architecture their protocols are not normally used to define and introduce a particular communication architecture.

As an additional remark, we should understand that combinations of different level protocols are not always possible or at least cannot be classed as simple and trivial problems. For example, MQTT is created to operate over TCP/IP, and without radical modifications, it may not be used over a UDP/IP stack [11].

1.2 Security in wireless transmission

It is a known fact that since wireless systems are based on a broadcast nature they are vulnerable to interferences. Despite a general comprehension that only suspects the top and bottom layers of the OSI model to be subject to

Fig. 3.2: Attack examples on OSI model layers.

security complexities, all the levels may be manipulated or suffer from unauthorized access, in other words, been *attacked*. Some examples of dissimilar layer attacks are visualized in figure 3.2.

As it is shown, attacks or interferences can happen everywhere in the transmission encapsulation procedure. Starting from application level, which is in charge of data request specifications as well as interactions with the end-users, next to the packets encryption and trustworthy transfer in the transport layer, and after that the network layer which creates connections between routers by using IP addresses all the way down to the MAC and PHY layers.

The types of attacks on each levels are different in nature and some important remarks are listed as bellow:

- Application layer attacks are mostly malware interferences that refer to malicious software in form of codes written by the attacker to interrupt the normal transmission paradigm or steal information.

- Transport layer attacks are normally in the type of flooding attacks. These generally belong to the category of denial of service (DOS) attacks, which send huge number of ping requests and consequently flood the input and output buffer of the nodes.

- Network and MAC layer attacks are mainly spoofing or hijacking attacks that generate illegitimate IP address to mask the identity of the attacker that tends to harm the transmission network.

- PHY layer attacks mostly happen in terms of jamming attacks that can block a single or a sweep of multiple frequencies in a communication channel.

Further explanations on wireless security issues and attack types along with detection schemes and countermeasures can be found in [73–80].

2 MQTT

In the research that resulted in this dissertation, MQTT is selected as the messaging level protocol. MQTT is considered as a lightweight messaging protocol based on its publish/subscribe methodology and being suitable for low power, and low throughput applications [11, 81]. The main reasons for choosing this protocol over other widely used protocols for instance HTTP, or CoAP are summarized as stated bellow:

- Since MQTT is formed on publish/subscribe methodology, it provides a better level of *"plug and play"* characteristic in comparison to other protocols like HTTP or CoAP that are request/response systems. This is because a user can be seamlessly added to the structure and listen to the ongoing traffic without the requirement of implementing any changes to the operating system. To rephrase it, a one to may communication architecture can be easily designed by using MQTT protocol [11].

- Caused by the same reason, MQTT may be reckoned as a lower power protocol since, unlike the request/response protocols that require a continuous listening server MQTT structure is event-based [11].

- MQTT header formatting and structuring are designed with the intention of preserving bandwidth and computational resources. Due to this fact, MQTT may be better choice for systems with lower power elements like MG structures or IoT platforms [11].

Moreover, MQTT supports three degrees of quality of service (QoS) to provide dissimilar levels of message delivery reliability while sacrificing some bandwidth and adding to the overall latency. This is important when in an application the reliable delivery of a particular message is much more important than rapid messaging such as online banking transactions. The procedure and message structuring of different MQTT-QoS levels are provided at figure 3.3. As one can see, higher QoS means more transmissions are necessary for one single successful message delivery which translates to larger latency [11].

The other important aspect of the MQTT structure is the employment of a broker which acts as a communication server and all the messages are relayed through this unit prior to being delivered to the respected subscribers. The broker also provides useful decoupling features between *subscribers & publishers* which contributes to seamless user adding or removing and is demonstrated at figure 3.3.

The are several MQTT brokers that may be selected to be employed for creating MQTT platforms. For this study, **Eclipse Mosquitto**™ is selected which is one very popular and widely implemented open source broker [82].
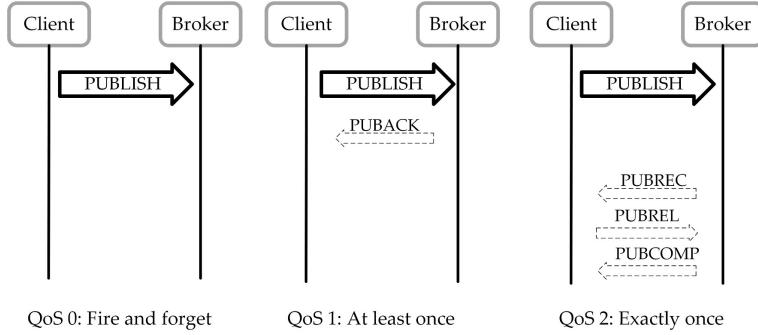
Fig. 3.3: MQTT QoS levels.

Mosquitto broker is light and may be accommodated by low computational resourceful devices like Raspberry Pi mini-computers. On the downside, Mosquitto does not offer sophisticated security measures and only authentication and user authorization are provided [11, 82].

3 MG communication and control system description

To achieve the formerly mentioned objectives of this thesis detailed models for both systems, control and messaging, are required so that the integration challenges and issues can be addressed and evaluated.

3.1 Electrical model

The electrical MG is modeled on a setup that consists of four fully bidirectional 2.2 kW inverters from *Danfoss*, LCL filters, a *DS1006* processor unit from *dSPACE*, and measurement cards [83]. A picture of the setup is provided in figure 3.4.

Founded on the characteristics of this platform different MG architectures can be modeled and tested. For this work, a GC residential MG formed by the methodology of GFD converters is designed and implemented into the setup. It is worth noting, the control models are created in SIMULINK and transferred to the dSPACE unit. In this suggested architecture, three inverters are utilised for different MG elements modelling as described below:

- **Inverter one:** emulates the load by receiving active power setpoints from an off-site profile generator and regulating its power output accordingly. The load data is 24 hours electricity consumption of a typical residential MG, synthetically generated based on real data.

Fig. 3.4: Experimental setup in AC-MG lab, Aalborg University.

- **Inverter two:** emulates PV electricity generation and the methodology is similar to inverter 1, however, the power flow directions are opposite to each other.

- **Inverter three:** emulates an ESS by utilising a battery model and performing SoC calculations.

The inverters share a common DC link provided by a REGATRON programmable DC supply. On the AC side, they are attached to a transformer and subsequently the stiff grid by a PCC.

The general idea of this model is to simulate a smart building as a home-like MG for futuristic applications. This smart home contains its own power station (PV panels) and aims to decrease the energy trade with the main network as much as possible by including an ESS. This ESS, which is interfaced to the smart home bus through a GFD inverter, requires power setpoints to perform charge and discharge actions. In this model, these power

setpoints are calculated in an external EMS, therefore bidirectional communication links are required to couple the different elements, that are load, PV generation, and ESS, with the EMS.

3.2 Communication model

In regard to the MG electrical model described above the communication framework should be designed to provide bidirectional links between the MG elements, consumption, generation, and ESS to the EMS. As indicated previously, the MG elements are emulated on *Danfoss* inverters coordinated by a dSPACE unit. Therefore, the communication module for the inverters is needed to be attached to the dSPACE card. This may not be regarded as a trivial problem since dSPACE units only support low-level communication through serial ports so modifications are required. Conversely, the EMS is hosted by a personal computer, therefore, enabling wireless messaging capabilities is more straightforward.

Regarding the communication protocols, so far, we decided that the transmission system will be founded on MQTT as the top layer protocol. In addition, WiFi (IEEE 802.11) is chosen to physically connect the units because of its compatibility with MQTT and additionally the available LAN of the lab that the experimental setups are situated. So, in line with the MQTT basics we need to couple the MG elements with MQTT users and create an MQTT broker to complete the network.

As previously mentioned, the main challenge is to create an MQTT node for the inverters through the dSPACE system. This node was created by coding **Pycom/Lopy4** microcontrollers in micropython and connecting them to the DS1006 card through its serial port. To make this connection possible, a **MAX3232** adapter is also required to convert the UART logical levels of the **Lopy4** device to **RS232** levels that are understandable for the dSPACE device. The wiring and connectivity of **Pycom/Lopy4** and **MAX3232** units are represented at figure 3.5 [11].
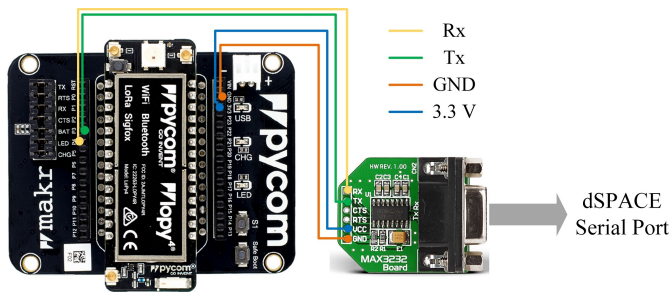

Fig. 3.5: Lopy4 and MAX3232 connection wiring.

It is necessary to note that a data conversion and also an addressing mechanism are required for the abovementioned combination. Initially, the payloads of the MQTT frames must be extracted and converted from their initial single precession float representations to four-byte hexadecimal format so that they can be transferred through the low-level transmission class of the serial channel. Besides, since the dSPACE unit is controlling multiple inverters an addressing mechanism is also required that adds a byte to the frame identifying the proper address of the message since the dSPACE unit controls multiple inverters. Likewise, another byte is also included highlighting what is the type of the setpoint since it is also possible to relay reactive power setpoints in our model. Briefly speaking, every MQTT frame received by the **Pycom/Lopy4** is converted to an *array of six bytes* and then relayed to the DS1006. Transmission from the other direction (from dSAPCE to the microcontroller) follows the same methodology but in the opposite direction. The conversion and addressing mechanism are visualized in figure 3.6.

The overall combination of the MQTT modules created on **Pycom/Lopy4** devices into the inverters' control architectures is shown in figure 3.7. Moreover the MQTT node for the EMS was created using the identical methodology as described above.

Besides, the Mosquitto MQTT broker, [82], was created on an affordable and simple **Raspberry Pi** computer to serve the low-power and low-cost ideology.

3.3 MG Architecture

Once the electrical and messaging models are designed the MG outline can be represented. As previously explained, this architecture contains both con-
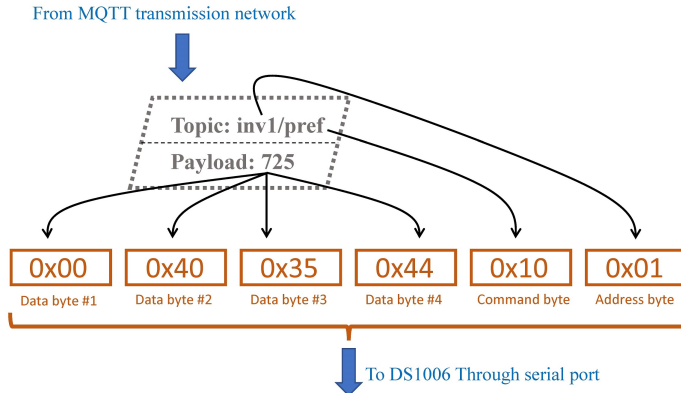
Fig. 3.6: Data conversion and addressing system in **Pycom/Lopy4** microcontrollers.
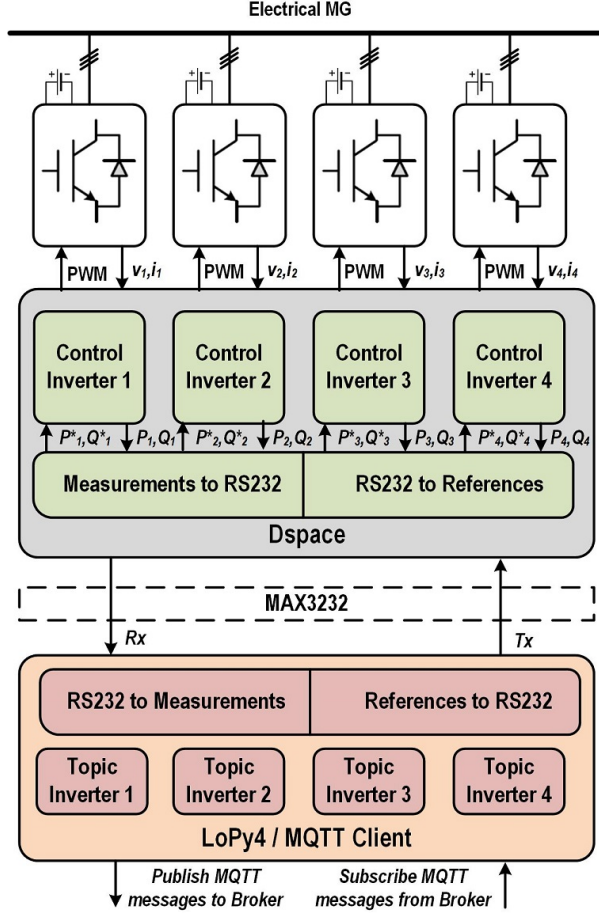
Fig. 3.7: MQTT communication node for smart inverters.

trol and messaging structures, and the integration validation and challenges are about to be investigated and analysed. This proposed architecture is visualized in figure 3.8 where the MQTT transceiver nodes can be noticed. These nodes and their operational responsibilities are:

1. Inverters, publish power measurements and ESS SoC. Subscribe to EMS power setpoints and also load/PV generation profiles from the profile generator.

2. EMS, publish active power setpoints for the storage unit. Subscribe to active power readings from the inverters.

3. Profile Generator, publish load/PV consumption profiles for *(Inverter*
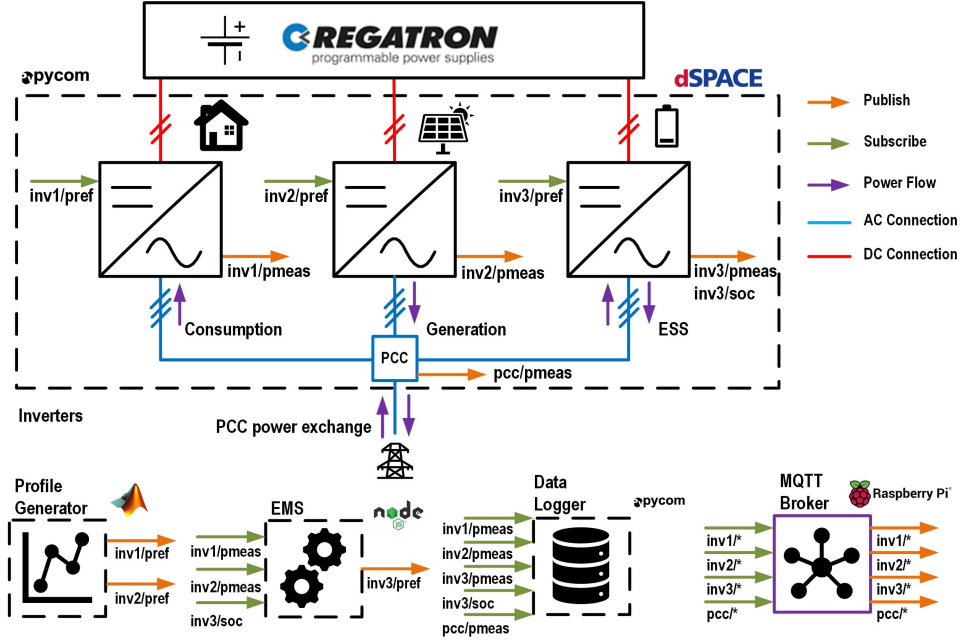
Fig. 3.8: MG proposed architecture.

#1 and #2)

4. Data Logger, subscribes to all the published topics and record the data for post-analysis.

Additionally an illustration of the GFD control algorithm for the inverters *(Inverter #1-3)* is provided at figure 3.9. It is possible to observe, this control structure consists of a current loop and a power loop to consume power references and regulate the outward active power accordingly. In addition, a power calculator block is included, which is combined with the MQTT module. This block calculates the instantaneous active power values and subsequently transmits these measurements to the MQTT Node to be published over designated topics.

Furthermore, a phase-locked loop (PLL) is added in the model so that the voltage magnitude and the frequency of the converter can be adjusted in a way that synchronisation with the power network is achieved.

4 Experimental validation and Results

This is a list of experimental tests that are conducted and enclosed in this part of the report to verify the aforementioned MG concept architecture [11]:
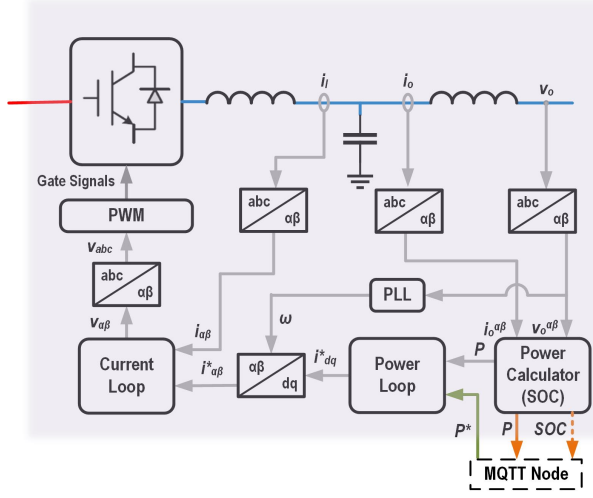
Fig. 3.9: GFD control schema for converters.

1. MQTT latency tests.

2. Power following tests for the inverters due to their received setpoints.

3. PCC electricity trades and ESS operational status tests for normal and abnormal (large latencies of failures) communication system situations, namely, MG energy management tests.

Every one of these tests are explained in detail as follows:

4.1 Latency tests

In the direction of finding out the serviceability of the planned messaging system for the aforementioned application, from the transmission speed viewpoint, MQTT overall delay values are evaluated in this part. To quantify the MQTT latencies the following steps are conducted:

- Two **Pycom/Lopy4** units are coded in micropython to act as MQTT transceivers. A broker was created on a **Raspberry Pi** to complete the messaging network.

- The **Pycom/Lopy4** internal clocks are synchronised to a same NTP server. (*Pool.ntp.org*)

- Each message is timestamped before transmitting from *Node 1* and this timestamp is relayed to *Node 2* by sending it as the packet payload. The packet is timestamped again after being recognized (received) by *Node 2*.

- 350 messages, in 5 seconds intervals, are transmitted from *Node 1*. Since the actual payloads are transmission timestamps, *Node 2* has access to both send and receive timestamps and record the data on a comma-separated values (.CSV) archive. It is worth noting that in these tests the payload size is *20 bytes* for every transmission.

The outcome is summarized in figure 3.10. It is worth noting, the experiment was conducted for *QoS-0* as-well-as *QoS-1* and as it may be clearly seen the latencies are larger when the transmissions are made more reliable (*QoS-1*) as expected.
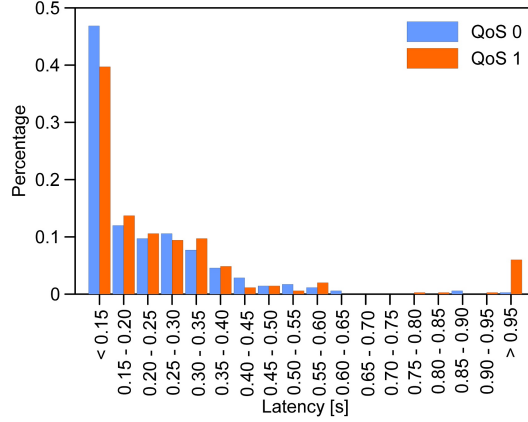
Fig. 3.10: Latency measurements for QoS-0 & QoS-1.

As another remark, in accordance with the recorded test values, MQTT cannot be classed as a fast-enough network for very quick synchronisation-level control scenarios like secondary control of MGs based on GFM converters. However, for transferring power setpoints of GFD inverters that are more energy management class problems, MQTT may be a feasible candidate since in these applications the messaging cycles are several seconds and in some situations considerably more.

As previously mentioned the payload length is fixed in the forenamed tests that is in accord to a single numeric value transmitted. Nevertheless, it is also important to analyse the impact of dissimilar payload sizes on the latency values of MQTT. To achieve this goal, the same test configuration as before is employed but this time different payload sizes consisting of one, ten, one hundred, one thousand, two thousand, and four thousand numeric figures were transmitted, and the latencies are recorded. An average of ten transmissions are calculated and presented as the outcome of the experiment, which is visualized in figure 3.11 and listed in table 3.1.

From the above results it may be concluded that adding the length of the payload in an MQTT frame will not affect the delays noticeably until the TCP
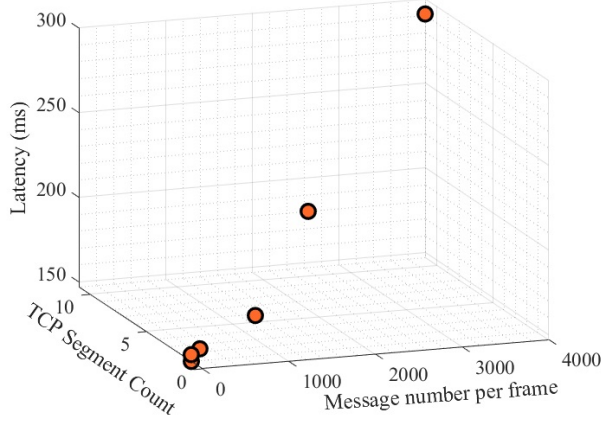
Fig. 3.11: Impact of payload size on MQTT latency.

Table 3.1: MQTT transmission latencies for dissimilar payload length.

Payload length (*byte*)	21	89	418	4017	8016	16018
Delay (*sec*)	0.147	0.151	0.154	0.161	0.205	0.291
TCP Segments	One	One	One	Three	Six	Eleven

segment byte limit is reached (*1500 bytes in our LAN configuration*). When the number of TCP segments are increased (from one thousand messages and above) the delays grow as expected until a large 0.291 (*sec*) delay for the case of four thousand numeric values in a single frame.

4.2 Power following tests

These tests aim to verify if the GFD converters, that are utilized in the architecture displayed at figure 3.8, can actually follow the externally transmitted power setpoints. To rephrase it, the implemented control system visualized at figure 3.9 is about to be validated now.

The test is conducted by forming an MQTT network similar to the one employed for the previous tests. For this reason, one independent **Pycom/Lopy4** is commanded for transmitting random power setpoints and also receiving the inverter's power measurements and recording the data on a (.CSV) file. Another **Pycom/Lopy4** was applied to create an MQTT node for the smart inverter succeeding the methodology provided in figure 3.7.

A fresh active power setpoint is generated every 2 minutes and the sampling intervals are every 5 seconds. The test duration was 30 minutes, and the findings are displayed at figure 3.12.

Some observations and results are gathered from this experiment.

- All the relayed setpoints are recognized by the inverter since the sensory readings match the setpoints. This firstly means the transmission system is **operating properly** and secondly the control algorithm can **regulate the actual power accordingly**.

- There is one mismatch point at about second 1100, which is because of the occurrence of a transient effect. To be specific, at this particular instance the fresh setpoint is recognised by the inverter but the output was not fully adjusted to that reference value.

As a broad remark, this test validates the effective and accurate combination of the designed MQTT network with the control algorithm of GFD inverters for the handling and coordination of our specific GC-MG framework.

4.3 MG energy management tests

After presenting that the inverters can receive externally generated power references and adjust their active power accordingly now the MG energy management is being studied as a whole. In this part of the report, added to presenting the duty of a healthy communication system on MG internal power adjusting, the harmful effects of large delays and in the worst-case total failures are investigated and contextualized. The tests in this part are compartmentalized as follows:

1. Energy management tests with healthy communication system.

2. Effects of sizeable delays.

3. Full messaging system failure impacts.
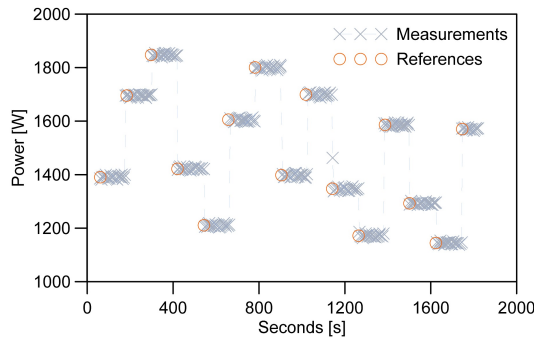
Fig. 3.12: Power following test results.

The First Case - Operational Links: Considering the architecture displayed at figure 3.8 the test methodology is described as bellow:

- Load and generation profiles, [11], are transmitted to inverters #1 and #2 through the MQTT network (**MQTT topics:** *inv1/pref* and *inv2/pref*). The datasets are for 24 hours with 1 minutes resolution.

- The EMS receives output active power readings of those two inverters along with the battery model SoC (**MQTT topics:** *inv1/pmeas, inv2/pmeas,* and *inv3/SOC*). Based on these inputs, power setpoints for the storage system are worked out and transmitted (**MQTT topic:** *inv3/pref*).

- The logger subscribes to all the measurement related topics and record the data for post analysis.

The first results are provided in figure 3.13, where the load and generation (solar PV) power readings are plotted for the test time-interval. In the next plot, figure 3.14, the battery power values and the instantaneous SoC measurements are represented. It is worth noting, the battery is assumed to be fully drained at the start of each day. Finally, and more notably, the energy trades with the power network for both scenarios of **with** and **without** operational transmission system is displayed at figure 3.15.
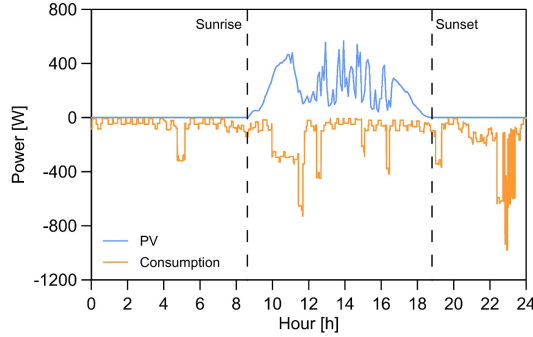
Fig. 3.13: Consumption and PV-generation measurements for 24-hours test interval.

The outcome of an operational EMS on the energy localization of MGs can be comprehended from figure 3.15. As it may be observed, if the EMS does not operate properly, large amounts of energy are traded with the network since production and load never fully match. However, if the EMS operates acceptably (which translates to a functioning messaging network), the energy trades are mostly limited to transient peaks and the power transaction is minimised. Further details of this experimental test and numerical results may be located in [11].
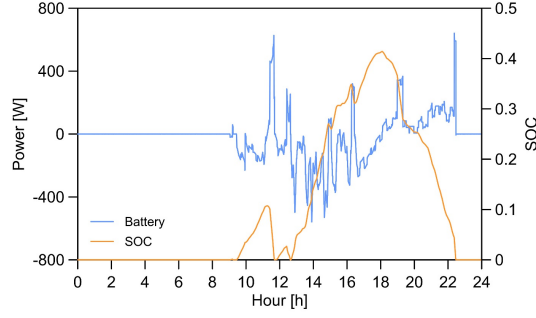
Fig. 3.14: Battery power and SoC measurement values.
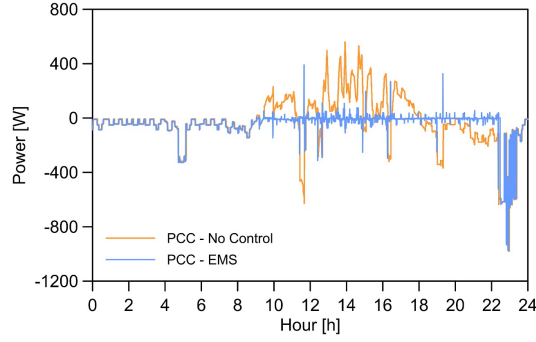
Fig. 3.15: PCC power trades.

The Second Case - Large Delays: Findings of the latency tests prove that the nominal overall latency levels are mostly fewer than 300 milliseconds, figure 3.10. However, large delays may occur in less efficient messaging systems due to different reasons such as MAC congestion situations, low-throughput PHY layers, or even some types of cyber-attacks.

Here, the impacts of relatively large latencies are examined on the effectiveness of the emulated MG. These latencies are formed by packet bouncing [11]. In the first case, five-second delays are introduced on the data stream and the PCC activities are monitored for a five-minutes period, figure 3.16.

After observing the effects of five-second latencies, other latency levels, namely, 0.5, 5, 10, and 30 seconds are also tested to figure out how much these delays can influence the deviation of the system from its inside energy equilibrium. The outcome is summarised in figure 3.17 and as it may be comprehended in an interval of 30 minutes even 30 seconds delays (which are huge) result in much fewer energy trades in comparison to the no-communication scenario.

(a) Overall

(b) Single PCC exchange detail.
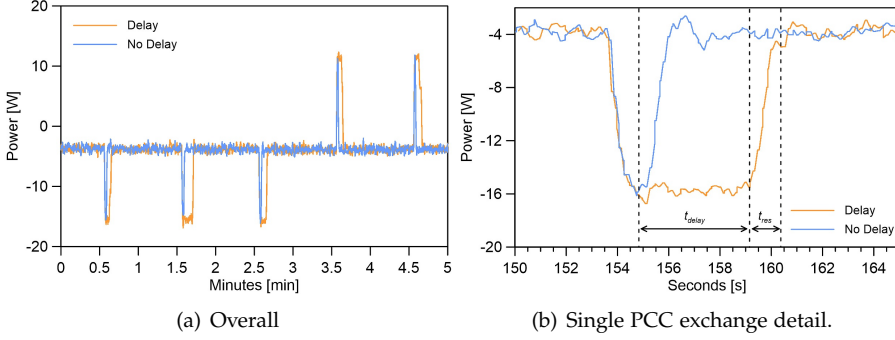
Fig. 3.16: PCC power trades with five-second latencies.
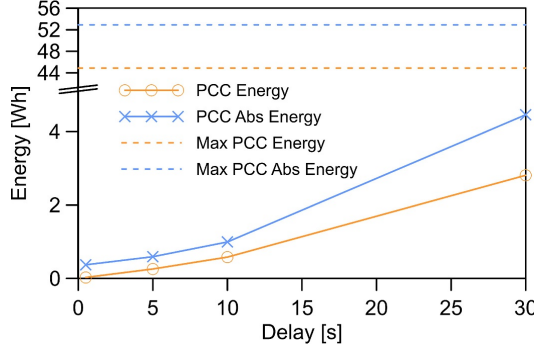
Fig. 3.17: Energy trades with the power network for 0.5, 5, 10, and 30 second intentional link latencies.

The Third Case - Link Failures: If a total communication link-outage occurs in the aforementioned structure the ESS becomes literally deaf, losses its smartness feature, and henceforth continues to run with its latest power setpoint. To simulate these situations, during a thirty minutes time period, a link outage is planned to occur after 10 minutes. The network recovers after minute 20 and continues to operate for another 10 minutes. The power trades with the electrical network and the storage system power values are visualized at figure 3.18.

As previously stated, and may be comprehended from figure 3.18(b), when the transmission network is out the ESS continues to work with its final received setpoint which is 140 Watts and is charging. This may cause harmful, overcharge problems if the battery reaches to fully charged status in the span of the fault. Thus, it is more reliable to equip the ESS with a safety algorithm that can shut it down (alter the setpoint to zero) if the fault's duration passes a certain threshold.

(a) Normal operation.

(b) Fault at minute 10, recovery at minute 20
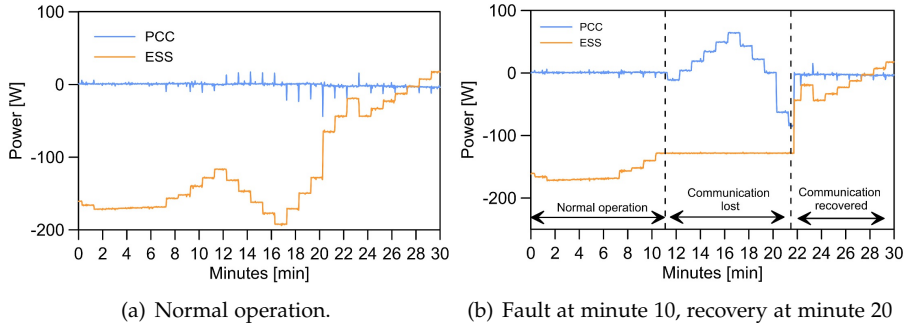
Fig. 3.18: Power trades with the electrical network and battery power values for healthy and faulty network status.
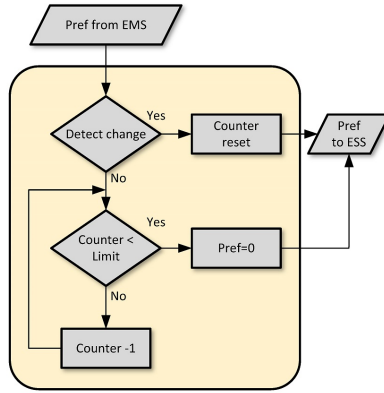
Fig. 3.19: ESS safety algorithm.

The flowchart of this safety algorithm is provided in figure 3.19 and the system response with the safety measure activated after 5 minutes of the fault occurrence is visualized at figure 3.20.
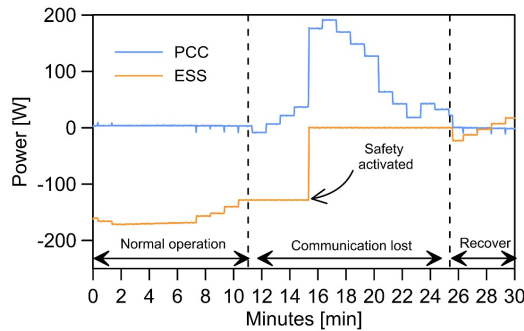
Fig. 3.20: Power trades with the grid and battery power reading with safety system.

41

As it may be clearly seen, the storage system setpoints are changed to zero after the safety measure is employed, and although the power trade is not optimum the battery integrity is conserved.

4

Communication infrastructure for MG scenarios with widely separated units.

I n this chapter, MG scenarios are considered where the elements are spread on wide areas and conventional short-range PHY protocols, like WiFi, cannot successfully create required links between devices. However, in communication engineering, the terms wide coverage cannot be accurately defined and is open to interpretation. Generally speaking, if the coverage exceeds a hundred meters, the network is not a LAN any longer and may be recognized as a wide area network (WAN). A classification of network types and PHY protocols is visualized in figure 4.1 [44].
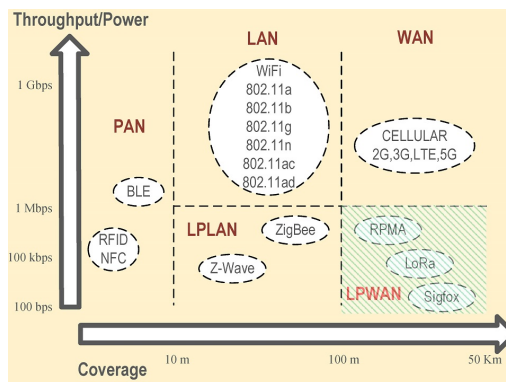
Fig. 4.1: Wireless networks and PHY protocols.

In this illustration, both coverage and throughput are provided so a useful comparison between different protocols may be established. In this figure, a couple of less famous network types are also included which are LPLANs and also LPWANs. The key convergence point of these two sorts of networks is their lower operational energy consumption when compared with conventional technologies which is accomplished by sacrificing throughput. Because of the low-power characteristic, these protocols may be deployed in small and affordable battery-powered IoT class transceivers.

In this division of the thesis, we are more interested in LPWANs since they may be employed when there are large separation distances between MG units. For instance, a remote PV module, or a wind turbine in an exurban houselike MG scenario. By way of illustration, the main idea of this part of the study is outlined in figure 4.2.
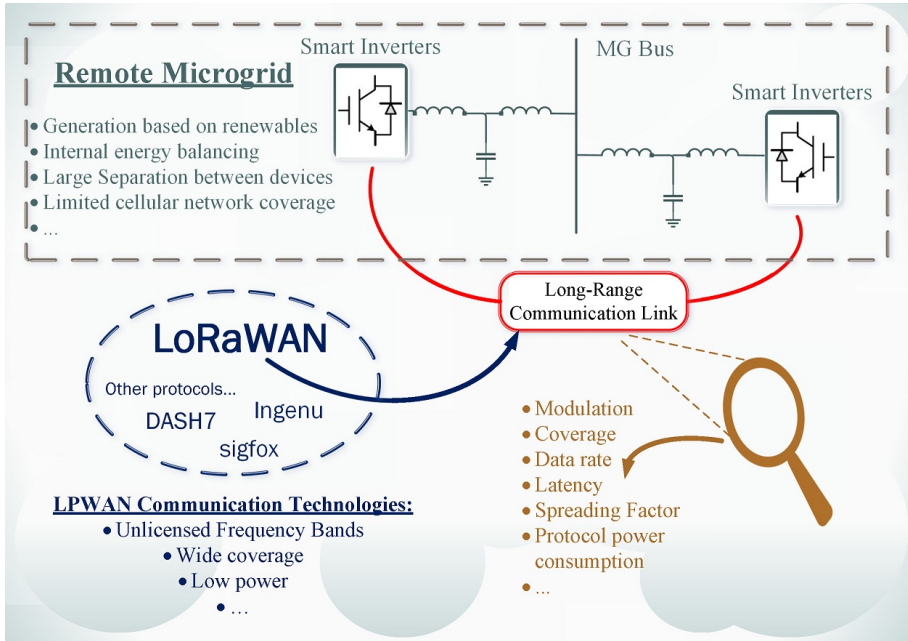
Fig. 4.2: A study on transmission networks for MG scenarios with widely spread units.

1 LPWAN protocols

These communication systems are developed to fill the gap amongst wireless LANs and cellular networks, where the former lacks extended coverage and the latter has accessibility issues together with high capital and operational

expenses. Different protocols are created that fit in this classification of M2M messaging frameworks and they all share some key characteristics [44]:

- Normally, unlicensed frequency channels are employed to avoid extra registration payments.

- The coverage is about several kilometres.

- The whole messaging architecture and methodology are founded on the power conservation idea. This results to low-throughput links and low energy end-devices.

Some well-established LPWAN protocols are *LoRaWAN, SigFox, Ingenu,* and *Dash7* and each of those present some benefits and suffer from some disadvantageous. Hence, there is not a general guideline for preferring one over the rest and the selection relies on the specific application, budget, and geographical considerations [44].

Founded on the brief descriptions provided earlier it might be declared that, LPWANs are comparable to private LANs (like WiFi) that transmit over unlicensed frequencies with cellular-level coverages. To rephrase it, LPWANs and cellular networks are rivals for widespread M2M applications.

Among various LPWAN technologies, LoRaWAN is one of the pioneering works and more-recognized names. At the same time, NB-IoT is a familiar M2M protocol structured over LTE networks. Consequently, it is worth conducting a simple comparison betwixt the features of these protocols. This may assist to comprehend the basic differences of these two classes of networks, figure 4.3 [44].
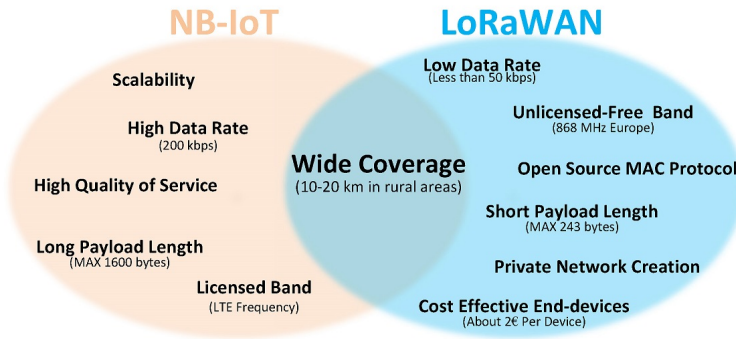
Fig. 4.3: LoRaWAN vs NB-IoT.

As it is known, the process of choosing one category over the other greatly relies on the requirements and if the application does not demand ultra-high throughput channels and contrastingly forming private networks are more

favorable, LoRaWAN may be regarded as a better choice than NB-IoT or other cellular M2M frameworks.

2 LoRa & LoRaWAN

These two terms represent different concepts; however, they are occasionally mistaken and subsequently misused. Therefore, here they are distinguished by the following definitions:

- Proprietary LoRa is a PHY protocol. Its modulation technique is chirp spread spectrum (CSS) and transmissions take place over 868/915 MHz bands.

- LoRaWAN is a MAC protocol and is open source.

In this research, LoRa is the selected protocol to provide smart inverters with long range capabilities and loRaWAN is utilised to form a hybrid messaging network for rural MG scenarios. Comprehensive details on the applications of these protocols for intelligent systems is gathered in [44]. Additionally, the CSS technique specifications and mathematical representations are comprehensively discussed in the same article, [44].

2.1 Spreading factor

An important feature of LoRa is the capability to select dissimilar spreading factors (SFs). The idea of SF in LoRa is thoroughly explained in [44]. Very briefly speaking, SF indicates the time on-air (ToA) of LoRa frames, and the higher the SF more time is needed for a specific frame transmission. The concept is visualized in fig 4.4 where an identical message is repeatedly transmitted by LoRa with unalike SFs. These frames are acquired by an ADALM-PLUTO SDR device programmed in SIMULINK to provide spectrogram presentations [44].

Thus far the significance of increasing SFs is comprehended. It is worth noting that, leaving aside the three SFs displayed in figure 4.4 SF7, SF8, and SF9 may also be employed. Now, it is time to address the question of why it is necessary to increase the SF levels that as previously mentioned contribute to more ToA and consequently less link throughput? The answer is in accord with the wider coverage which may be attained by using higher SF levels. The logic for this is rather simple when the SF level is increased the ToA elevates and the transceiver on the reception side may gain more chances to analyse the transmitted signal and consequently the frame can be successfully recognized and captured in longer distances [44, 84]. This may be translated

(a) SF10   (b) SF11   (c) SF12
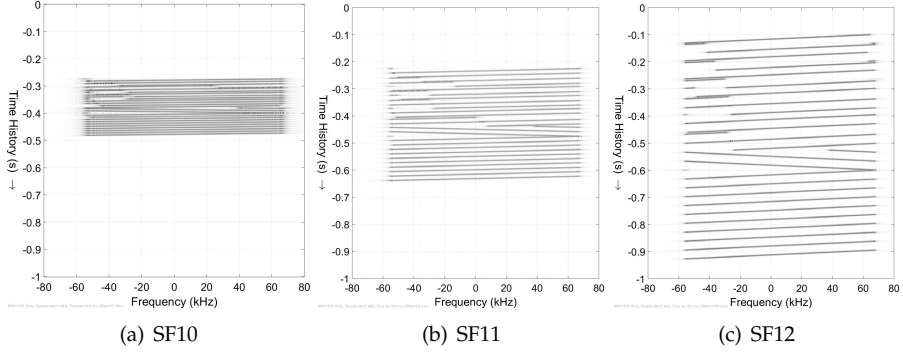
Fig. 4.4: Impact of dissimilar SFs on the ToA of LoRa frames. *LoRa Bandwidth 125 kHz, 868 MHz Channel*

Table 4.1: LoRa channel Throughput for dissimilar SFs. *LoRa Bandwidth:125 kHz*.

SF :	7	8	9	10	11	12
Throughput (*bps*)	6835	3906	2197	1220	671	366

as higher reception sensitivity that is *-137 dbm* for SF12 while it is only *-123 dbm* for SF7, which shows a considerable difference and can affect the coverage substantially [84].

Nevertheless, despite wider coverage, larger SFs also denote higher communication energy consumption along with being slower so the SF should be configured with care and consideration with accord to the requirements and specification of each application.

2.2 ToA measurements

The previously mentioned ToAs with accord to the employed SFs were experimentally evaluated by using two LoRa transceivers created on **Pycom/Lopy4** devices. To achieve an accurate ToA value for each SF the average ToA of five hundred transmissions with four-second intervals were calculated and the outcomes are gathered in figure 4.5.

The methodology of measuring these ToAs are almost identical to latency measurements of MQTT described in section 4.1, by calculating the difference between transmission initiation, and frame received recognition timestamps. Detailed explanations in this regard, including theoretical ToA calculations and comparisons to experimental results are gathered in [44].

Directing attention to these results verify that the ToA approximately doubles by moving to a higher SF which increases the reviver sensitivity but reduces the throughput as calculated and presented at table 4.1.
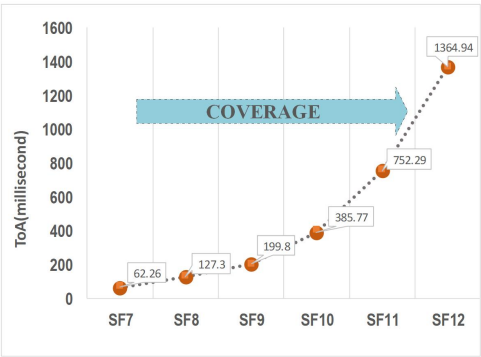
Fig. 4.5: LoRa transmission ToA for various SFs. Payload size: twenty bytes.

2.3 LoRa coverage field-test

To better explain the impact of dissimilar SFs on a LoRa network coverage a field-test was conducted by using two **Pycom/Lopy4** radios where the first one is acting as a sender the other as a receiver and logger. This experiment was conducted in AAU campus. Five separation situations between these two units were evaluated and each time fifty frames (*with 20 bytes payload size,*) were transmitted and logged. Afterwards, the packet delivery ratios (PDR) were calculated, and the outcomes are listed in table 4.2. The test configuration is also outlined in figure 4.6.

Fig. 4.6: LoRa coverage field test layout. Payload size: twenty bytes - *Image source:Google Maps, Aalborg University campus.*

The results in table 4.2 clearly show the impact of employing dissimilar SFs on the PDR of LoRa transmission. As it can be comprehended, SF7

Table 4.2: LoRa field test results. *LoRa Bandwidth:125 kHz, Tx power: 14 dBm.*

	1	2	3	4	5
PDR-SF7	100%	75%	None	None	None
PDR-SF12	100%	100%	100%	8%	100%
Remarks	Same room	Adjacent building	Ground floor	Ground floor	12 story tower

provides only short-range although it may still be stronger than LAN protocols. Contrariwise, SF12 gives very high reviver sensitivity, and frames are captured in distances that are way beyond LAN type technologies. It is important to note that in the positioning situation presented in the last column in which the separation distance is about six hundred meters the transmitter was positioned on the 12th floor and that affects the PDR substantially. This highlights the importance of establishing a clear line-of-site path between the transmitters in LoRa networks.

3 Smart inverters integrated with LoRa nodes

In line with the previous discussions of this chapter, LoRa can be contemplated as a feasible solution for providing inverters with long range, low energy, and affordable messaging features. Here, an experimental model is presented that was developed and tested to validate such an implementation. The model is outlined in figure 4.7.

The hardware that is employed to emulate the MG is the same setup that was utilized before and was described in section 3.1. As it may be clearly seen in figure 4.7, a LoRa receiver/transmitter developed on a **Pycom/Lopy4** microcontroller is attached to the DS1006 processor that controls the inverters and the electrical MG structure, this is denoted as **LoRa Node-A**. In such manner, the inverters can communicate to outside units through LoRa. Another LoRa device was developed on a similar microcontroller to form a point-to-point LoRa network with the inverter. The second LoRa device, denoted as **LoRa Node-B**, was also programmed to be MQTT compatible so that it can participate (*publish & subscribe*) in an active MQTT network, hence it must be WiFi enabled.

There are some highlights regarding the communication framework of figure 4.7 which are listed bellow:

- *868 MHz* frequency channel is employed with *125 kHz* bandwidth.

- LoRa Node-A is attached to the DS1006 processor by the RS232 port which is comparable to the system described in section 3.1.

- LoRa Node-B is also participating in an MQTT network. The payload of LoRa frames are extracted and MQTT messages are created and pub-
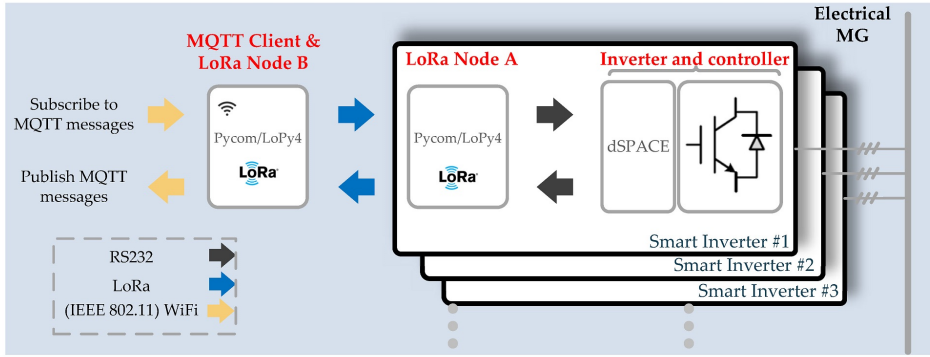
Fig. 4.7: Smart inverters' communication framework based on LoRa.

lished (for received LoRa frames from Node-A). A similar process is followed for transmission from Node-B to Node-A. In this respect, Node-B may be recognized as a LoRa/MQTT gateway.

- Three PHY protocols are participating in this messaging framework.

- No LoRaWAN architecture is implemented, the connection between LoRa Node-A & Node-B are strictly point-to-point LoRa transmissions.

By utilizing the explained framework several benefits may be attained:

- Long-range messaging feature is achieved for inverters since LoRa PHY is used. Therefore, the system has the competency of controlling and coordinating widespread DGs of an MG framework.

- If the communication modules attached to the units are powered by batteries, they can stay alive for long periods (maybe years in some configurations) since LoRa is a low-power protocol.

- The capital and operational expenses are low, because LoRa transceivers are created on affordable devices and registration fees are not required for LoRa frequency band usage.

- The LoRa/MQTT gateway provides the possibility to provide heterogeneity, and also expanding the network easily. This is convenient to integrate HMIs for monitoring, or management & coordination algorithms that may be hosted by user-friendly platforms (Android, MAC, and Windows) since they all can be made MQTT compatible.

The previously explained messaging mechanism from **LoRa Node-A** towards **LoRa Node-B** (or LoRa/MQTT gateway) can be better clarified if it is visualized in a flowchart, figure 4.8.

4 Experimental validation and results

A variety of tests are carried out to exemplify the usefulness of the suggested messaging structure previously described. The tests are designed with the following aims in mind:

- Firstly, it is intended to show the validity of the messaging network by displaying that the inverters are able to keep up with the remotely created power setpoints. It is worth noting, the inverters' control algorithm is no different from previous tests described in section 3.1 and
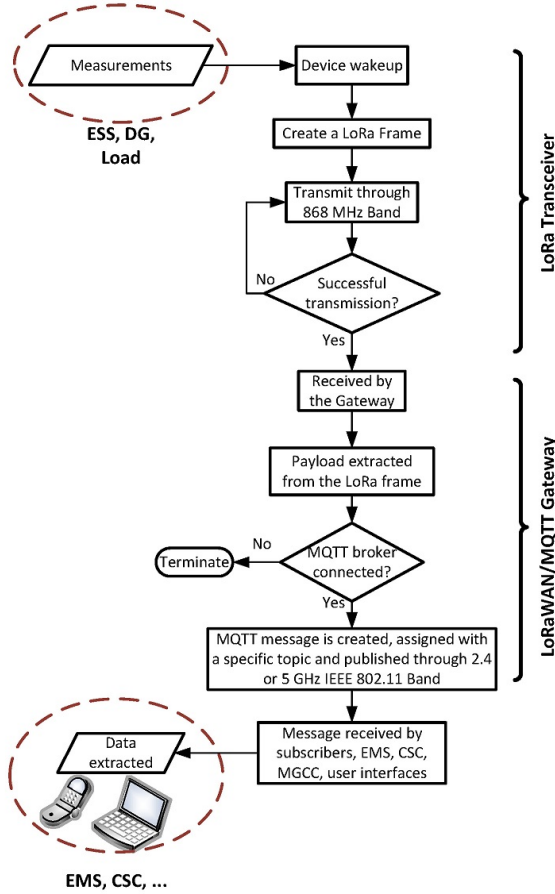
**Fig. 4.8:** Messaging mechanism between **LoRa Nodes-A & B**
.

visualized at figure 3.9.

- Secondly, the influence of different SF levels on the valid reception of messages is intended to be evaluated.

- Finally, the result of changing broadcasting power on the correct delivery of frames are to be presented.

Test A description   In this scenario **LoRa Node-A** and **LoRa Node-B** are positioned in different buildings and the distance between them is about one hundred meters, this emulates a real-world LoRa application since LAN wireless PHY protocols are not capable of handling the transmissions in these situations. The tests parameters are listed as bellow:

1. Ten **randomly generated** power setpoints with one-minute intervals are generated by a **MATLAB MQTT client** and published under the topic *inv/pref*.

2. **LoRa Node-B**, subscribes to this topic (*inv/pref*), extracts the payloads, creates LoRa frames and transfer the setpoint over LoRa. (*LoRa frequency:868 MHz, LoRa BW:125 kHz, Tx power:14 dBm, SFs: 7 & 12*)

3. **LoRa Node-A**, receives the frames, extract the messages and transfer the setpoints to the converters control structure hosted by the DS1006 processor through UART. (*UART Baud-rate: 115200 bauds, UART character: 8 Bits*)

4. **LoRa Node-A**, collects the inverter's power measurement by the same serial channel and transfers them back to **LoRa Node-B** through LoRa. Measurement sampling rates are five-second.

5. **LoRa Node-B**, gathers the measurements from received frames and publish them under MQTT topic *inv/pmeas*.

6. **A logger device**, which is coupled with the same MQTT server (broker), subscribes to all MQTT topics (*inv/pref & inv/pmeas*) and record the data on a .CSV file for post analysis.

The setpoint following results are visualized in figure fig31. As shown, when SF12 is selected, which means larger ToA, all the setpoints are recognized, and the output powers are adjusted accordingly. This proves the supremacy of LoRa from conventional LAN protocols like WiFi, bearing in mind that the units are well separated and placed in two different buildings with various obstacles like doors and concrete walls. If the devices were placed even further apart, for instance, a couple of kilometres, with

an obstacle-free line-of-sight, the results would be the same since what is important on the signal strength and the receiver sensitivity is the link budget.

Contrastingly, in the event of SF7, figure 4.9(b) it may be noticed that some setpoints are lost (3rd, 7th, 8th, and 10th) and there are periods that the link fails which proves SF 7 may not be identified as a proper option for how the sender and receiver are positioned in this test configuration. The outcome clearly demonstrates the influence of dissimilar SFs on the range and robustness of the messaging link.

(a) SF12   (b) SF7
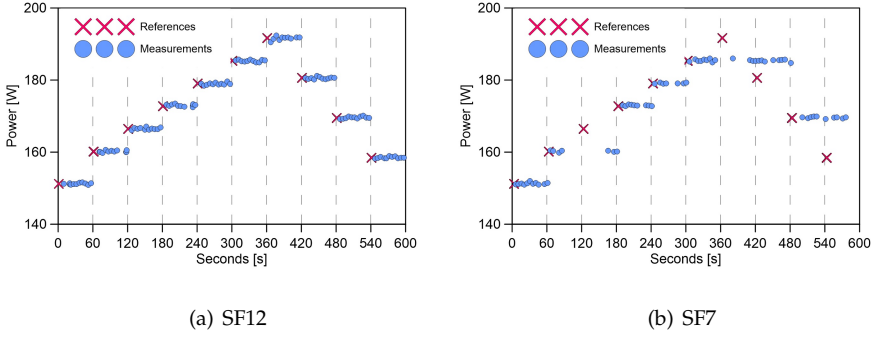
Fig. 4.9: LoRa setpoint following results, SF7 & SF12

(a) Tx 15(dBm)   (b) Tx 5(dBm)
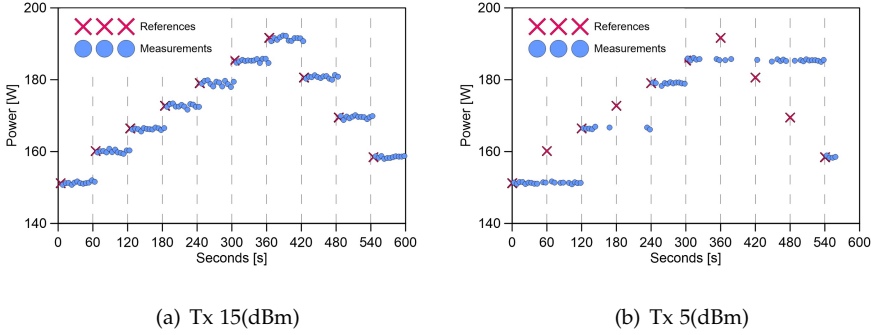
Fig. 4.10: LoRa setpoint following results, different transmission powers.

Test B description Test B is similar to test A in accord with the number and interval of the transmission. Besides, the methodology of the tests are identical and the participation of the units are the same. The difference is, however, in test B two different values for **transmission power** are examined

while in test A the outcomes of two **SFs** are contrasted. Additionally, in test B the physical gap between **LoRa Node-A & B** is reduced, and the radios are positioned in the same room (approximately ten meters apart with some typical lab obstacles). Since the influence of larger SFs on the coverage is already presented in test A, SF7 is employed for this test. The outcomes are visualized in figure 4.10.

As expected SF7 with a transmission power of 15 (dBm) provides satisfactory results, bearing in mind that the default Tx transmission power of LoRa is 14 (dBm). Nevertheless, in the event of decreasing the power to 5 (dBm), the link breaks up at some instances which proves that if LoRa parameters are not configured properly the network may become even less effective than normal LAN protocols bearing in mind that the devices are positioned closely and well in range of LAN protocols. To rephrase it, LoRa can only be considered a long-range protocol if the network variables such as: *SF, Tx power, BW, and frequency band*, are configured carefully.

Chapter 5

Communication link-loss effects mitigation

W e know that a transmission network which is employed to control and manage a smart system can malfunction, similar to any other communication system, because of various and different reasons. No matter the origin of these failures, or if they are deliberate or accidental when they occur the optimal performance of the smart system will be harmfully affected.

In this chapter, firstly, the link-loss influences on the efficacy of MGs are described. This is in accord with the kind of the control algorithm and how communication is employed in this structure. Afterwards, a solution for a more effective messaging architecture is proposed that is founded on load and generation short-term forecasting. The methodology for these forecastings based on neural networks is presented and discussed subsequently. Finally, the MG performance while employing the enhanced messaging algorithm is shown and examined by simulations.

1 Detrimental link loss effects on MG optimal performance

The consequence of a link malfunction on the behaviour of an MG strongly relies on the communication dependency of the particular MG architecture. These aspects were thoroughly covered in section 1 so it is redundant to be further explained in this part of the thesis.

Here, those aforesaid harmful effects of link malfunctions on the systematic behaviour of a GC-MG with GFD converters are numerically explained.
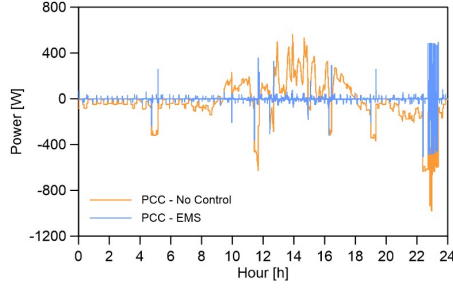
Fig. 5.1: MG power trades with the stiff grid when the messaging link is properly working (PCC-EMS) and malfunctioned (PCC-No control).

By employing the MG model and messaging system outlined in section 3.1 and the dataset introduced in section 4.3 a link malfunction experiment for a twenty-four hour period is conducted. The consequence of having a properly functioning transmission system on the power trade with the stiff grid is demonstrated in figure 5.1.

The numeric values of the results are arranged at table 5.1. It is worth noting that, the current experiment is dissimilar from the comparable tests explained in section 4.3 since in this instance the storage system is 100% charged at the starting point to demonstrate link-loss effects more concisely. It is imperative to highlight that, positive values indicate power injected into the electrical network while minus signs indicate imported power from the network.

Table 5.1: Numerical representation for communication malfunction consequences on proper operation of a grid-tied MG architecture equipped with a fully charged ESS and an off-site EMS.

	Consumption	Generation	Grid exchange Operational link	Grid exchange Failed link	% Difference
Energy [kWh]	-2.599	2.145	0.019	-0.455	-104.2
Ave Power [kW]	-0.116	0.089	0.002	-0.027	-92.6
Max Power [kW]	-0.980	0.567	0.492	0.560	-12.2
Min Power [kW]	-0.006	-0.001	-0.509	-0.980	-48.1

The results arranged in table 5.1 lead to some important understandings as listed below:

- The accumulated demand and production in the experiment period are not equal. This conveys that either a storage device is required, or a secondary supply (grid connection) should be included to offset this inequality.

- When the messaging network is functional, which implies the storage device receives proper power setpoints, the energy trade with the net-

56

work is only 0.019 kWh (exported to the electrical network). However, a complete link collapse changes this value to a considerable amount of 0.455 kWh (imported from the electrical network). This presents a large difference and highlights the benefit of including a storage device in an MG that is communication dependant as previously explained.

- The other rows of the table represent power trade indicators with the electrical network and demonstrate the same changes as the energy results.

To summarize this test and the respected outcomes, it may be declared that in the forenamed MG framework, which is GC and founded on GFD control algorithms, if the messaging link fails, preserving internal MG energy is not feasible anymore. This may result in grid and MG power quality issues, powerline over designs, and other related problems.

Proposed solution: To alleviate the aforesaid link loss complexities an innovative remedy is to design the MG & EMS architecture in a way that the ESS can anticipate its future power setpoints. To be specific, *by forecasting load and generation for upcoming time steps, the EMS may work out and transmit predicted setpoints to the storage unit and these anticipated values can be used if it becomes disconnected because of a messaging system malfunction.*

So, the first step is to find a solution for performing short-term forecasting of demand and generation, which will be unveiled in the succeeding section.

2   Short-term Load/Generation forecasting by Deep Learning (DL) methods

Demand and generation predictions for power systems scenarios such as MGs may be regarded as time-series forecasting problems that can be successfully addressed by multiple techniques. The majority of these methods are developed on DL approaches and some related studies are published in [85–87].

Founded on a thorough literature review on this topic, it has been comprehended that recurrent neural networks (RNN) and specifically long short-term memory (LSTM) algorithms may be regarded as decent methods for short term, time-series forecasting and can be employed for the specific scenario of this study [88]. Details of LSTM-RNN are well-acknowledged and may be extracted from the current literature, [89]. The general idea of LSTM is visualized in figure 5.2 where the relationships with the preceding steps are clearly shown.
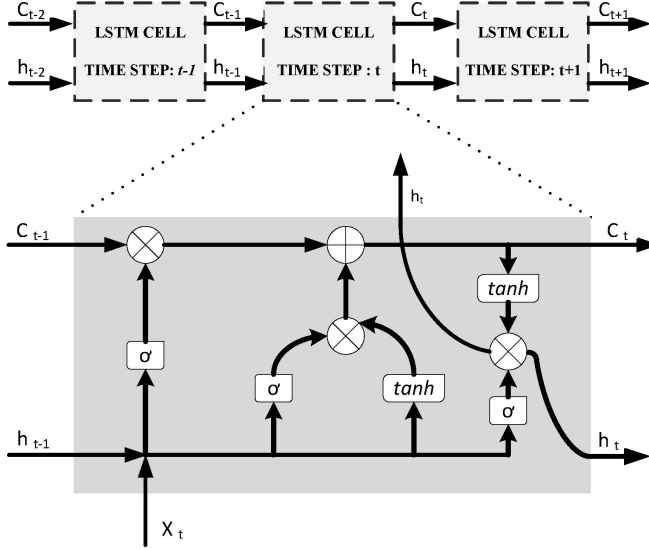
Fig. 5.2: LSTM-RNN
.

2.1 Short-term Load forecasting

To exhibit the capability of the LSTM-RNN algorithm for load forecasting in residential applications a data set consisting of thirty hours of consumption with one-minute time-steps is utilized, this dataset is taken from a formerly published study [11, 90]. The prediction methodology consists of training the neural network for twenty-nine hours and forecasting for the renaming hour which is conducted by using various **number of hidden layers and epoch numbers**.

In this manner, very short-term consumption forecastings are achieved and the outcomes are visualized in figure 5.3 and 5.4. It is worth noting that in figure 5.3 the neural network is updated with accurate data at each time step while in figure 5.4 forested figures are used for updates at each instance. To rephrase it, in the process of providing a forecasted value for every step, the previous hidden state (along with the previous cell state) that is required for the LSTM methodology, is obtained from the test-set data for the cases of figure 5.3, while the test-set values do not contaminate the network in the other case predictions visualized in figure 5.4.

From the illustrations some understandings can be extracted:

- The forecastings presented in the different configurations gathered in

(a) *Total hidden units:50, Epoch numbers:250 Training time(minutes): 0:49*

(b) *Total hidden units:50, Epoch numbers:500 Training time(minutes): 1:33*

(c) *Total hidden units:100, Epoch numbers:250 Training time(minutes): 2:00*

(d) *Total hidden units:100, Epoch numbers:500 Training time(minutes): 3:37*

(e) *Total hidden units:300, Epoch numbers:250 Training time(minutes): 12:56*

(f) *Total hidden units:300, Epoch numbers:500 Training time(minutes): 25:32*
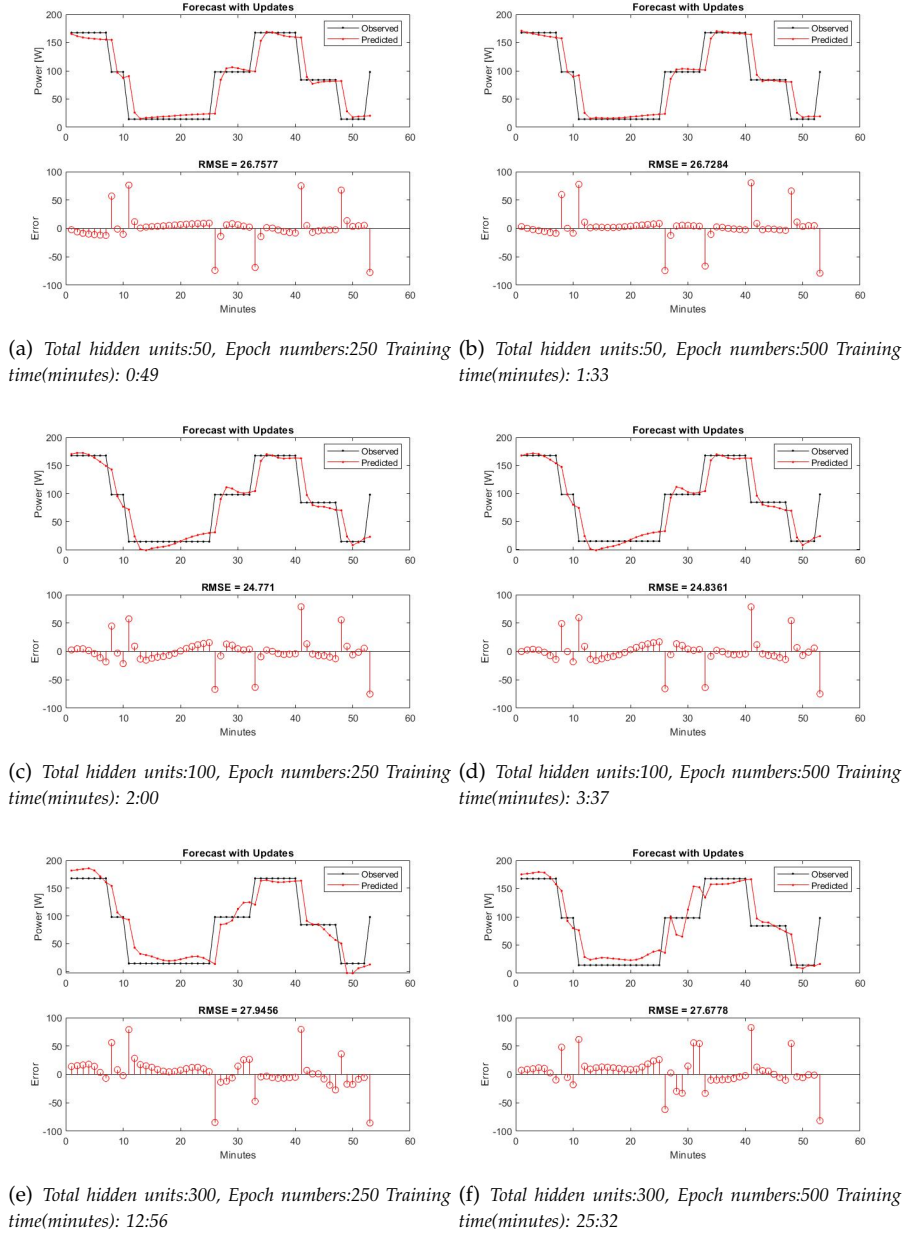
Fig. 5.3: Very short-term load forecastings for some different configurations. For each step, accurate data from the test-set is used as the previous hidden state to update the LSTM network.

(a) *Total hidden units:50, Epoch numbers:250 Training time(minutes): 0:49*

(b) *Total hidden units:50, Epoch numbers:500 Training time(minutes): 1:33*

(c) *Total hidden units:100, Epoch numbers:250 Training time(minutes): 2:00*

(d) *Total hidden units:100, Epoch numbers:500 Training time(minutes): 3:37*

(e) *Total hidden units:300, Epoch numbers:250 Training time(minutes): 12:56*

(f) *Total hidden units:300, Epoch numbers:500 Training time(minutes): 25:32*

Fig. 5.4: Very short-term load forecastings for some different configurations. For each step, predicted values are employed as the previous hidden state to update the LSTM network.

figure 5.3 seem to be very accurate, which is the case for all of them. However, as explained before, since accurate data from the test set is used to update the LSTM cells at each step these may not be regarded as realistic predictions for several time steps.

- In figure 5.4 it might be detected that in the situation of using fifty hidden units (a) & (b), disregarding the number of iterations, the forecasted curves cannot accurately follow the exact values since the network is not trained properly. All the same, by using too many hidden units, (e) & (f) the outcomes are not acceptable as well and this is owing to the training overfitting phenomenon. Therefore, a decent configuration can be **100-hidden units and 500-number of epochs** considering the pattern following, and the low root means square error (RMSE) values. Nevertheless, a strict rule-of thumb is not accessible in this regard and different configurations can also provide acceptable fittings.

2.2 Short-term generation forecasting

By employing the similar methodology of the preceding sets of forecastings, short-term predictions are conducted for PV generation. For this purpose, ten days of solar data, [1], is utilized and visualized in figure 5.5. The training is organized for nine days and the final day is predicted subsequently. Since the influences of properly configuring the neural network are previously explained, in this part only the selected configurations, which are **200-hidden units and 1000-epochs** are visualized in figure 5.6.

As it might be spotted, the forecast trend follows the actual data closely and the RMSE value is acceptable in regard with the data. Therefore, these
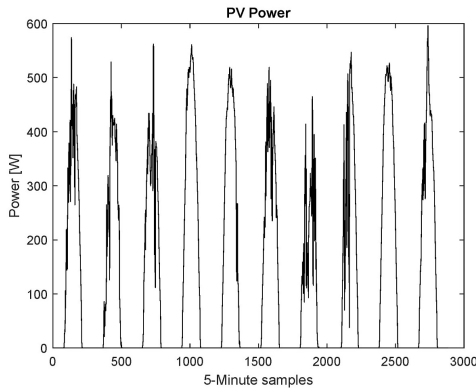
Fig. 5.5: Solar power generation data from NREL, [1]
.

predictions may be effectively employed for calculating future time-steps for the storage device.

3 Enhanced messaging system with forecasted setpoints

After showing how DL methods and specifically LSTM-RNN may be employed to accomplish short-term predictions on load and generation time-series, at this part a modified EMS is proposed that can utilize these predictions to produce scheduled enhanced messages (EM) to load the storage device with information about future. This methodology is outlined at figure 5.7 and as it is shown two distinct units (*EMS & ESS Pref Controller*) are collaborating to handle the storage unit power setpoints.

The important highlights of this architecture are stated as bellow:

- The EMS, calculates instantaneous power setpoints upon receiving demand and PV power measures. Since the profile time-steps are one-minute the setpoints are generated once per minute accordingly.

- It is scheduled to generate an EM every thirty minutes. Each message contains setpoints for the preceding hour with five-minutes increments.

- The *Pref Controller* firstly checks the health condition of the messaging link by searching for periodic changes in its revived value. Then, classify a received message as normal or enhanced, and finally, works out the proper storage system power setpoint for every time instance.

(a) Forecast (b) Forecast with updates
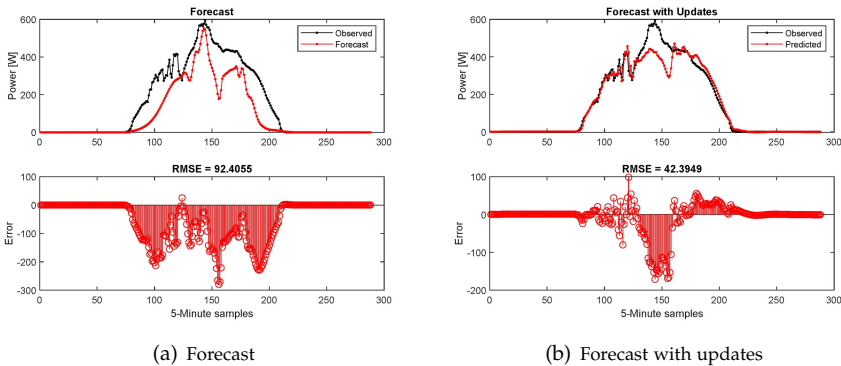
Fig. 5.6: Short-term solar forecastings *Number of hidden units:200, Epoch number: 1000.*
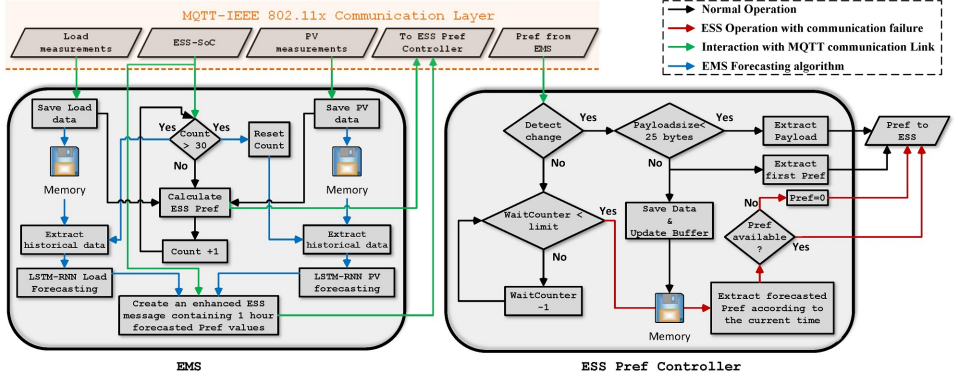
Fig. 5.7: Storage system messaging management.

- The link between these devices is an MQTT messaging network while they are physically linked by WiFi. These sorts of messaging systems are exhaustively described, and their effectiveness is experimentally validated in [11].

4 Simulation results

To exhibit the efficacy of the forenamed architecture of figure 5.7 a number of tests are conducted. Initially, *one hour* of the datasets employed in the tests of section 2 is separated and the MG energy inequality is calculated, which is *0.4367 (kWh)*. This means, if the setpoints are not updated, because of a link collapse, *0.4367 (kWh)* is traded with the stiff grid that may also be represented as *0.4464 (kW)* RMSE if zero PCC exchange is regarded as the no-error situation. The forecasted figures are also presented for these data and the outcomes are gathered in figure 5.8.

	1	2	3	4	5	6	7	8	9	10	11	12
Real-Time	356	281.4	302.4	387	486.6	527.6	552.6	469	405.4	397.4	493	581.6
Forecast	246.7	251.5	281	326.7	384.6	420.6	413.1	397.9	401.6	423.2	456.8	487
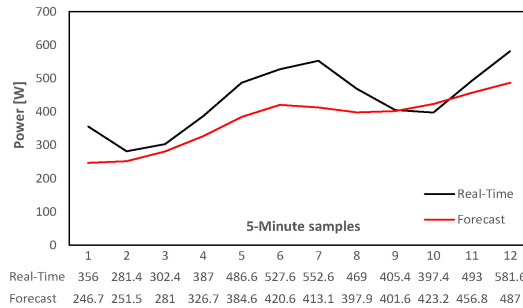
Fig. 5.8: Load and generation power inequalities for the MG in one hour. Accurate and forecasted representations are provided.

The forecasted trend in figure 5.8 shows that the predictions pattern may closely follow the actual data while not being a hundred percent accurate as expected. In this instance, it is time to numerically evaluate the consequence of a link breakdown in two cases. Recalling the forenamed system specifications, an EM is planned to be aired every thirty minutes. This means two extreme failure situations may exist:

1. Link-loss happens instantly **after** an EM is received.

2. Link-loss happens just **before** an EM is received.

These two situations are visualized in figure 5.9, and each link-loss is lasting for a full hour.
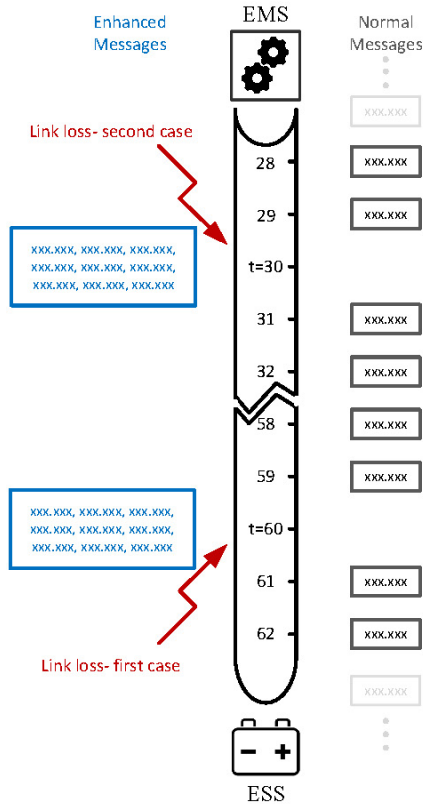
Fig. 5.9: Link-loss extreme scenarios

.

The important difference between these two fault situations is in the former forecasted power setpoints are available for the entire fault period while in the latter these setpoints are only provided for half of the malfunction duration. This is in regard to the methodology of the EM formation that contains data for the preceding hour. It is worth noting that, in accordance with the algorithm of the *Pref Controller* if a setpoint cannot be found for a particular step the storage device closes up to avert harmful operations.

The outcomes of these experiments, in respect of calculated errors between forecasted and accurate power setpoints, that can exhibit the efficacy of our proposed modified EMS are displayed in figure 5.10.

(a) First case   (b) Second case
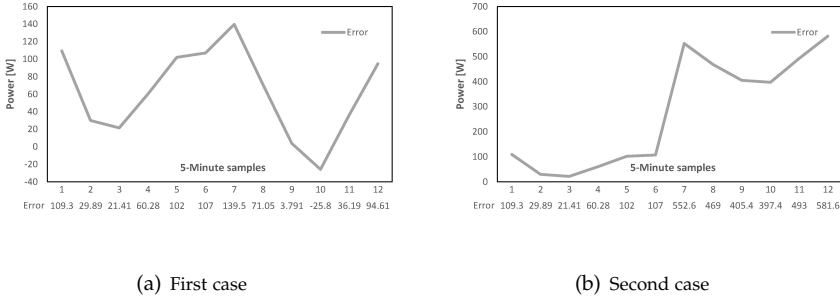
Fig. 5.10: Error between predicted and accurate storage system power setpoints for two fault cases.

The results show that in the first fault scenario *0.0624 (kWh)* is traded with the electrical network that may also be represented as *0.0273 (kW)* RMSE. This shows a huge improvement from the basic situation (link-loss and no forecasted setpoints are provided for the battery) explained before. In the other scenario *0.2774 (kWh)* is exchanged, which is still much improved from the basic system, however, the MG is less efficient than the preceding scenario.

Chapter 6

Conclusion

In the final part of this thesis, a summary of the different aspects discussed in the preceding chapters is provided followed by a highlighting of the primary contributions of the research. In the end, a few future trends that are expected to expand this research will be mentioned.

1 Summary

This thesis was started with an introduction that generally explained M2M transmission frameworks and their role in MG management and control. In the introduction, some different MG architectures were introduced, and it was explained that the duty of the transmission link differs in accord with the class of the power system. To put it another way, the contribution of communication in MG management cannot be strictly defined and it strongly relies on the control algorithm characteristics. IoT and CPS ideas were also spoken of in the introduction since an MG architecture with an integrated messaging framework may be regarded as an example of either of these concepts. A brief summary of M2M messaging protocols and technologies was also included in the introduction to draw attention to the availability of various transmission networks with different characteristics. In addition, it was highlighted that there are dissimilar levels and layers in MG models from the communication point of view that are very different in respect of characteristics as well as requirements. However, the focus of this study is more on two of the aforesaid layers (*Smart-home level & MG level*) and the others are out of the scope at this instance.

The concept of smart inverters (**Paper A**) was introduced in the second chapter including discussions about their important smartness indicators and

most importantly the proper messaging protocols that may be employed for these devices. Besides, in this chapter *smart inverters* are conceptualized, and this was crucial since the next parts of this dissertation are based on these types of instruments.

In the third chapter, (**Paper B**), a messaging system was modeled and integrated into a GC-MG architecture for PCC power trading management. For this purpose, MQTT which is a compact and practical messaging layer protocol was employed and its benefits with respect to similar technologies were discussed and highlighted. An experimental platform was designed by using industrial-grade devices for the electrical MG and the transmission architecture. It is worth noting that, no ready-to-use or pre-designed platform was employed for either of the forenamed systems. The implementation was experimentally validated for normal and abnormal (faulty) situations.

The duty of messaging links in MG coordination was further investigated in the fourth chapter where the benefits of using LPWAN technologies were described with regard to their long-range and low-power characteristics, (**Paper C**). LoRaWAN was selected as a proper messaging network for our application of concern among other LPWANs, respecting its particular specifications. A LoRa-enabled smart inverter was designed and inaugurated in this chapter and how it may be employed in an MG control architecture was demonstrated. The influence of different LoRa configurations on the system performance, in the matter of effective power setpoint following, was visualized by performing experimental tests.

Finally, a methodology for mitigating messaging link losses in MG systems was suggested in chapter five, (**Paper D-Submitted**). In this part, the harmful impacts of transmission link losses were initially introduced followed by the proposal of a more capable architecture that may assist to fade these potential problems. The method was founded on short-term load and generation forecastings by using DL learning techniques. The proposed framework of the modified EMS that was capable of generating enhanced messages loaded by future power setpoints was validated by providing simulation results.

2 Main contributions & Important findings

The main contributions of this PhD study and also its distinguishable points from similar research efforts are listed as follows:

- The practicability of implementing a weightless and user-friendly messaging system such as MQTT for management and coordination of GC-AC-MG systems is demonstrated and validated. These sorts of transmission systems are commonly regarded as IoT messaging protocols

and their exploitation into power system applications was not thoroughly investigated in previous works.

- The utilization of other kinds of PHY protocols that may allow for expanded coverage and consume lower transmission energies is investigated. These protocols, LPWANs, can be very useful when the separation distances between independent elements of a smart system are beyond the coverage of normal LAN protocols like WiFi. Specifically, LoRa and LoRaWAN are investigated and studied in this regard.

- In the setup employed for both communication PHY protocols, signal and data conversions were required to make the connection of the communication nodes to the DS1006 card achievable. This was a result of the utilization of the RS232 serial port on the dSPACE side. This connectivity also required an addressing procedure for both directions. To put it another way, a unique protocol was designed for this transmission (between the microcontroller-based transceivers and the inverters) in parallel to the primary considerations and findings of the research.

- Throughout the research, all tests and scenarios were investigated from both communication and control systems points of view, and this distinguishes this work from other related studies. To be specific, control architectures were coded in SIMULINK and messaging devices were created from scratch by micropython coding. Their integrations were also made possible by proper code lines either in SIMULINK or in python. To rephrase it, no ready-to-use local or web-based platform was employed to assist the integration and this may be considered as another factor that emphasizes the novelty of this study.

- The results prove that familiar messaging systems such as MQTT may be efficiently used for MG management. This is, of course, for the energy management class applications since their messaging intervals are in the range of seconds or more. Contrastingly, these communication links are not suited for very agile purposes like $V \& f$ synchronizations by secondary controllers.

- The strength and superiority of LoRa over conventional LAN technologies like WiFi in respect of coverage and energy consumption have been validated.

- Detrimental transmission links malfunction impacts on the proper functionality of MGs were analysed and discussed.

- The competency of LSTM-RNN as a member of DL methods for effective short-term time series forecasting for the required time horizon of

our MG application was demonstrated. It was proven that by employing a more intelligent EMS-ESS combination, that can anticipate future power setpoints, MG internal energy independence may be further accomplished and power trade with the stiff grid can be limited.

3 Future works

MGs are still at their initial and emerging state in real-world scenarios, and communication dependency is inevitable in these kinds of frameworks, therefore, lots of future trends, in very different directions, can be planned to follow the existing studies. Nevertheless, some directly related steps to this PhD study that are worth further investigation are listed here:

- Real-world emulations for the messaging architectures announced in this work should be conducted. In this manner, more realistic evaluations will be possible and unknown issues can be explored.

- Cellular-based M2M protocols and their comparison with LPWANs when integrated into power systems should be quantifiably investigated and analysed. These protocols can provide further possibilities due to their abundance bandwidth, higher resiliency, and reliability.

- Finding similar solutions for MG-related scenarios that require faster links such as $V \& f$ restorations by secondary control in islanded (or GC) MG architectures that are formed by GFM converters. As explained previously, the messaging frameworks that are designed and developed in this work are not suitable to deal with these sorts of applications.

- LPWANs are not very secure protocols. This is in accord with the trade-off between security measures and simplicity (thus lightweightness) in messaging systems. Nevertheless, the security cannot be overlooked and requires further investigation, keeping in mind that the protocols must still remain simple and low power.

References

[1] NREL, "Grid Modernization-Solar Power Data for Integration Studies." [Online]. Available: https://www.nrel.gov/grid/solar-power-data.html

[2] "Consumer vs Prosumer: what's the Difference?" 2017. [Online]. Available: https://www.energy.gov/eere/articles/consumer-vs-prosumer-whats-difference{%}0A

[3] R. Lasseter and P. Piagi, "Microgrid: A Conceptual Solution," *Proceedings of the 2004 IEEE 35th Annual Power Electronics Specialists Conference,,* vol. 38, no. 1, pp. 1–7, 2016.

[4] C. Marnay, S. Chatzivasileiadis, C. Abbey, R. Iravani, G. Joos, P. Lombardi, P. Mancarella, and J. Von Appen, "Microgrid evolution roadmap," in *Proceedings - 2015 International Symposium on Smart Electric Distribution Systems and Technologies, EDST 2015.* IEEE, 2015, pp. 139–144.

[5] F. Martin-martínez and M. Rivier, "A literature review of Microgrids : A functional layer based classi fi cation," *Renewable and Sustainable Energy Reviews*, vol. 62, pp. 1133–1153, 2016.

[6] J. Rocabert, A. Luna, F. Blaabjerg, and P. Rodríguez, "Control of power converters in AC microgrids," *IEEE Transactions on Power Electronics*, vol. 27, no. 11, pp. 4734–4749, 2012.

[7] A. Bidram and A. Davoudi, "Hierarchical structure of microgrids control system," *IEEE Transactions on Smart Grid*, vol. 3, no. 4, pp. 1963–1976, 2012.

[8] J. M. Guerrerol, N. Berbel, J. Matas, J. L. Sosa, and Luis Garcia de Vicufia, "Droop Control Method with Virtual Output Impedance for Parallel Operation of Uninterruptible Power Supply Systems in a Microgrid," in *APEC 07 - Twenty-Second Annual IEEE Applied Power Electronics Conference and Exposition*, 2007. [Online]. Available: http://ovidsp.ovid.com/ovidweb.cgi?T=JS{&}PAGE=reference{&}D=emed11{&}NEWS=N{&}AN=70992724

[9] J. M. Guerrero, J. C. Vasquez, J. Matas, L. G. De Vicuña, and M. Castilla, "Hierarchical control of droop-controlled AC and DC microgrids - A general approach toward standardization," *IEEE Transactions on Industrial Electronics*, vol. 58, no. 1, pp. 158–172, 2011.

[10] B. Arbab-Zavar, E. Palacios-Garcia, J. Vasquez, and J. Guerrero, "Smart Inverters for Microgrid Applications: A Review," *Energies*, vol. 12, no. 5, p. 840, 2019.

[11] B. Arbab-zavar, E. J. Palacios-garcia, and J. C. Vasquez, "Message Queuing Telemetry Transport Communication Infrastructure for Grid-Connected AC Microgrids Management," *Energies*, vol. 14, no. 18, p. 5610, 2021.

[12] Q. Shafiee, C. Stefanovic, T. Dragicevic, P. Popovski, J. C. Vasquez, and J. M. Guerrero, "Robust networked control scheme for distributed secondary control of islanded microgrids," *IEEE Transactions on Industrial Electronics*, vol. 61, no. 10, pp. 5363–5374, 2014.

[13] J. W. Simpson-Porco, Q. Shafiee, F. Dorfler, J. C. Vasquez, J. M. Guerrero, and F. Bullo, "Secondary Frequency and Voltage Control of Islanded Microgrids via Distributed Averaging," *IEEE Transactions on Industrial Electronics*, vol. 62, no. 11, pp. 7025–7038, 2015.

[14] F. Guo, C. Wen, J. Mao, and Y. D. Song, "Distributed Secondary Voltage and Frequency Restoration Control of Droop-Controlled Inverter-Based Microgrids," *IEEE Transactions on Industrial Electronics*, vol. 62, no. 7, pp. 4355–4364, 2015.

[15] X. Lu, X. Yu, J. Lai, J. M. Guerrero, and H. Zhou, "Distributed Secondary Voltage and Frequency Control for Islanded Microgrids With Uncertain Communication Links," *IEEE Transactions on Industrial Informatics*, vol. 13, no. 2, pp. 448–460, 2017.

[16] A. Bidram, A. Davoudi, F. L. Lewis, and J. M. Guerrero, "Distributed cooperative secondary control of microgrids using feedback linearization," *IEEE Transactions on Power Systems*, vol. 28, no. 3, pp. 3462–3470, 2013.

[17] Q. Shafiee, J. M. Guerrero, and J. C. Vasquez, "Distributed secondary control for islanded microgrids-a novel approach," *IEEE Transactions on Power Electronics*, vol. 29, no. 2, pp. 1018–1031, 2014.

[18] F. Guo, C. Wen, J. Mao, J. Chen, and Y. D. Song, "Distributed Cooperative Secondary Control for Voltage Unbalance Compensation in an Islanded Microgrid," *IEEE Transactions on Industrial Informatics*, vol. 11, no. 5, pp. 1078–1088, 2015.

[19] D. Wu, T. Dragicevic, J. C. Vasquez, J. M. Guerrero, and Y. Guan, "Secondary coordinated control of islanded microgrids based on consensus algorithms," *2014 IEEE Energy Conversion Congress and Exposition, ECCE 2014*, pp. 4290–4297, 2014.

[20] D. He, D. Shi, and R. Sharma, "Consensus-based distributed cooperative control for microgrid voltage regulation and reactive power sharing," *IEEE PES Innovative Smart Grid Technologies Conference Europe*, vol. 2015-Janua, no. January, pp. 1–6, 2015.

[21] A. Al-Fuqaha, M. Guizani, M. Mohammadi, M. Aledhari, and M. Ayyash, "Internet of Things: A Survey on Enabling Technologies, Protocols, and Applications," *IEEE Communications Surveys and Tutorials*, vol. 17, no. 4, pp. 2347–2376, 2015.

[22] M. R. Palattella, M. Dohler, A. Grieco, S. Member, G. Rizzo, J. Torsner, T. Engel, and L. Ladid, "Internet of Things in the 5G Era : Enablers , Architecture , and Business Models," *IEEE Journal on Selected Areas in Communications*, vol. 34, no. 3, pp. 510–527, 2016.

[23] I. Yaqoob, E. Ahmed, I. A. T. Hashem, A. I. A. Ahmed, A. Gani, M. Imran, and M. Guizani, "Internet of Things Architecture: Recent Advances, Taxonomy, Requirements, and Open Challenges," *IEEE Wireless Communications*, vol. 24, no. 3, pp. 10–16, 2017.

[24] C. Gomez, A. Arcia-Moret, and J. Crowcroft, "TCP in the Internet of Things: From Ostracism to Prominence," *IEEE Internet Computing*, vol. 22, no. 1, pp. 29–41, 2018.

[25] A. Čolaković and M. Hadžialić, "Internet of Things (IoT): A review of enabling technologies, challenges, and open research issues," *Computer Networks*, vol. 144, pp. 17–39, 2018.

[26] S. P. Mohanty, U. Choppali, and E. Kougianos, "Everything you wanted to know about smart cities," *IEEE Consumer Electronics Magazine*, vol. 5, no. 3, pp. 60–70, 2016.

[27] S. E. Collier, "The Emerging Enernet: Convergence of the Smart Grid with the Internet of Things," *IEEE Industry Applications Magazine*, vol. 23, no. 2, pp. 12–18, 2017.

[28] E. A. Lee, "Cyber physical systems: Design challenges," *Proceedings - 11th IEEE Symposium on Object/Component/Service-Oriented Real-Time Distributed Computing, ISORC 2008*, pp. 363–369, 2008.

[29] J. Lin, W. Yu, N. Zhang, X. Yang, H. Zhang, and W. Zhao, "A Survey on Internet of Things: Architecture, Enabling Technologies, Security and Privacy, and Applications," *IEEE Internet of Things Journal*, vol. 4, no. 5, pp. 1125–1142, 2017.

[30] M. Centenaro, L. Vangelista, A. Zanella, and M. Zorzi, "Long-range communications in unlicensed bands: The rising stars in the IoT and smart city scenarios," *IEEE Wireless Communications*, vol. 23, no. 5, pp. 60–67, 2016.

[31] Y. Mehmood, N. Haider, M. Imran, A. Timm-giel, and M. Guizani, "M2M Communications in 5G : State-of-the-Art Architecture , Recent

Advances , and Research Challenges," *IEEE Communications Magazine*, vol. 55, no. September, pp. 194–201, 2017.

[32] N. Naik, "Choice of effective messaging protocols for IoT systems: MQTT, CoAP, AMQP and HTTP," *2017 IEEE International Symposium on Systems Engineering, ISSE 2017 - Proceedings*, 2017.

[33] A. P. Foster, "Messaging Technologies for the Industrial Internet and the Internet of Things Whitepaper," *Prismtech*, no. March, pp. 1–22, 2014.

[34] M. Siekkinen, M. Hiienkari, J. K. Nurminen, and J. Nieminen, "How Low Energy is Bluetooth Low Energy ? Comparative Measurements with ZigBee / 802 . 15 . 4," pp. 232–237, 2012.

[35] H. Van Der Bent, "Wireless technology in industrial automation," *EngineerIT*, vol. 93, no. MARCH, pp. 30–31, 2010.

[36] A. Zaballos, A. Vallejo, and J. M. Selga, "Heterogeneous communication architecture for the smart grid," *IEEE Network*, vol. 25, no. 5, pp. 30–37, 2011.

[37] S. Tayeb, S. Latifi, and Y. Kim, "A survey on IoT communication and computation frameworks: An industrial perspective," *2017 IEEE 7th Annual Computing and Communication Workshop and Conference, CCWC 2017*, vol. 1301726, pp. 1–6, 2017.

[38] V. Bhuvaneswari and R. Porkodi, "The internet of things (IOT) applications and communication enabling technology standards: An overview," *Proceedings - 2014 International Conference on Intelligent Computing Applications, ICICA 2014*, pp. 324–329, 2014.

[39] P. P. Parikh, M. G. Kanabar, and T. S. Sidhu, "Opportunities and challenges of wireless communication technologies for smart grid applications," *IEEE PES General Meeting, PES 2010*, no. Cc, pp. 1–7, 2010.

[40] Z. Zhu, S. Lambotharan, W. H. Chin, and Z. Fan, "Overview of demand management in smart grid and enabling wireless communication technologies," *IEEE Wireless Communications*, vol. 19, no. 3, pp. 48–56, 2012.

[41] M. Kuzlu, M. Pipattanasomporn, and S. Rahman, "Review of communication technologies for smart homes/building applications," *Proceedings of the 2015 IEEE Innovative Smart Grid Technologies - Asia, ISGT ASIA 2015*, pp. 1–6, 2016.

[42] I. Froiz-míguez, T. M. Fernández-caramés, P. Fraga-lamas, and L. Castedo, "Design , Implementation and Practical Evaluation of an IoT home automation system for fog computing applications based on MQTT and Zigbee-wifi sensor nodes," *sensors*, pp. 1–42, 2018.

[43] A. Stanford-Clark and H. L. Truong, "MQTT For Sensor Networks (MQTT-SN) Protocol Specification," *International Business Machines Corporation (IBM)*, 2013.

[44] B. Arbab-Zavar, E. J. Palacios-Garcia, J. C. Vasquez, and J. M. Guerrero, "LoRa Enabled Smart Inverters for Microgrid Scenarios with Widespread Elements," *Electronics*, vol. 10, no. 21, 2021. [Online]. Available: https://www.mdpi.com/2079-9292/10/21/2680

[45] A. M. A.-M. Oratile Khutsoane, Bassey Isong, "IoT Devices and Applications based on Lora/LoRaWAN," in *IECON 2017 - 43rd Annual Conference of the IEEE Industrial Electronics Society*.

[46] A. Augustin, J. Yi, T. Clausen, and W. M. Townsley, "A Study of LoRa : Long Range & Low Power Networks for the Internet of Things," *sensors*, vol. 16(9), 146, pp. 1–18, 2016. [Online]. Available: https://doi.org/10.3390/s16091466

[47] S. Spinsante, G. Ciattaglia, A. D. Campo, D. Perla, D. Pigini, G. Cancellieri, E. Gambi, and A. S. Adriatica, "A LoRa Enabled Building Automation Architecture Based on MQTT," in *2017 AEIT International Annual Conference*, Cagliari, Italy.

[48] J. P. Thomesse, "Fieldbus technology and industrial automation," *Proceedings of the IEEE*, vol. 93(6), pp. 1073–1101, 2005.

[49] S. Vitturi, "On the use of Ethernet at low level of factory communication systems," *Computer Standards and Interfaces*, vol. 23, no. 4, pp. 267–277, 2001.

[50] T. Lennvall, M. Gidlund, and J. Akerberg, "Challenges when bringing IoT into industrial automation," *2017 IEEE AFRICON: Science, Technology and Innovation for Africa, AFRICON 2017*, pp. 905–910, 2017.

[51] J. A. Stankovic, T. F. Abdelzaher, C. Lu, L. Sha, and J. C. Hou, "Real-time communication and coordination in embedded sensor networks," *Proceedings of the IEEE*, vol. 91, no. 7, pp. 1002–1022, 2003.

[52] G. Cena, "An improved can fieldbus for industrial applications," *IEEE Transactions on Industrial Electronics*, vol. 44, no. 4, pp. 553–564, 1997.

[53] N. P. Mahalik and M. Yen, "Extending fieldbus standards to food processing and packaging industry: A review," pp. 586–598, 2009.

[54] E. J. Palacios-Garcia, J. M. Flores-Arias, A. Chen, F. J. Quiles-Latorre, and F. J. Bellido-Outeirino, "Home energy management system based on daily demand prediction and ZigBee network," pp. 315–316, 2015.

[55] J. Han, C. S. Choi, W. K. Park, I. Lee, and S. H. Kim, "Smart home energy management system including renewable energy based on ZigBee and PLC," *IEEE Transactions on Consumer Electronics*, vol. 60, no. 2, pp. 198–202, 2014.

[56] M. A. Setiawan, F. Shahnia, S. Rajakaruna, and A. Ghosh, "ZigBee-Based Communication System for Data Transfer Within Future Microgrids," *IEEE Transactions on Smart Grid*, vol. 6, no. 5, pp. 2343–2355, 2015.

[57] D. D. Olatinwo, A. Abu-Mahfouz, and G. Hancke, "A survey on LP-WAN technologies in WBAN for remote health-care monitoring," *Sensors (Switzerland)*, vol. 19, no. 23, pp. 1–26, 2019.

[58] A. Augustin, J. Yi, T. Clausen, and W. M. Townsley, "A study of Lora: Long range & low power networks for the internet of things," *Sensors (Switzerland)*, vol. 16, no. 9, pp. 1–18, 2016.

[59] J. Haxhibeqiri, E. De Poorter, I. Moerman, and J. Hoebeke, "A survey of LoRaWAN for IoT: From technology to application," *Sensors (Switzerland)*, vol. 18, no. 11, 2018.

[60] C. A. Hofmann and A. Knopp, "Direct access to GEO satellites: An internet of remote things technology," *IEEE 5G World Forum, 5GWF 2019 - Conference Proceedings*, pp. 578–583, 2019.

[61] J. M. Guerrero and Y. Xue, "Smart Inverters for Utility and Industry Applications," *PCIM Europe 2015*, no. May, pp. 277–284, 2015.

[62] Y. Shaoyong, X. Dawei, B. Angus, M. Philip, R. Li, and T. Peter, "Condition Monitoring for Device Reliability in Power Electronic Converters: A Review," *IEEE Transactions on Power Electronics*, vol. 25, no. 11, pp. 2734–2752, 2010.

[63] H. Oh, B. Han, P. McCluskey, C. Han, and B. D. Youn, "Physics-of-failure, condition monitoring, and prognostics of insulated gate bipolar transistor modules: A review," *IEEE Transactions on Power Electronics*, vol. 30, no. 5, pp. 2413–2426, 2015.

[64] J. O. Estima and A. J. Cardoso, "A new approach for real-time multiple open-circuit fault diagnosis in voltage-source inverters," *IEEE Transactions on Industry Applications*, vol. 47, no. 6, pp. 2487–2494, 2011.

[65] W. Zhang, D. Xu, P. N. Enjeti, H. Li, J. T. Hawke, and H. S. Krishnamoorthy, "Survey on fault-tolerant techniques for power electronic converters," *IEEE Transactions on Power Electronics*, vol. 29, no. 12, pp. 6319–6331, 2014.

[66] P. Lezana, J. Pou, T. A. Meynard, J. Rodriguez, S. Ceballos, and F. Richardeau, "Survey on fault operation on multilevel inverters," *IEEE Transactions on Industrial Electronics*, vol. 57, no. 7, pp. 2207–2218, 2010.

[67] C. Li, C. Cao, Y. Cao, Y. Kuang, L. Zeng, and B. Fang, "A review of islanding detection methods for microgrid," *Renewable and Sustainable Energy Reviews*, vol. 35, pp. 211–220, 2014. [Online]. Available: http://dx.doi.org/10.1016/j.rser.2014.04.026

[68] J. M. Guerrero, M. Chandorkar, T. L. Lee, and P. C. Loh, "Advanced control architectures for intelligent microgridspart i: Decentralized and hierarchical control," *IEEE Transactions on Industrial Electronics*, vol. 60, no. 4, pp. 1254–1262, 2013.

[69] J. M. Guerrero, P. C. Loh, T. L. Lee, and M. Chandorkar, "Advanced control architectures for intelligent microgridsPart II: Power quality, energy storage, and AC/DC microgrids," *IEEE Transactions on Industrial Electronics*, vol. 60, no. 4, pp. 1263–1270, 2013.

[70] S. H. Hu, C. Y. Kuo, T. L. Lee, and J. M. Guerrero, "Droop-controlled inverters with seamless transition between islanding and grid-connected operations," *IEEE Energy Conversion Congress and Exposition: Energy Conversion Innovation for a Clean Energy Future, ECCE 2011, Proceedings*, pp. 2196–2201, 2011.

[71] T. L. Vandoorn, B. Meersman, J. D. De Kooning, and L. Vandevelde, "Transition from islanded to grid-connected mode of microgrids with voltage-based droop control," *IEEE Transactions on Power Systems*, vol. 28, no. 3, pp. 2545–2553, 2013.

[72] N. Kakimoto, H. Satoh, S. Takayama, and K. Nakamura, "Ramp-rate control of photovoltaic generator with electric double-layer capacitor," *IEEE Transactions on Energy Conversion*, vol. 24, no. 2, pp. 465–473, 2009.

[73] Y. Zou, J. Zhu, X. Wang, and L. Hanzo, "A Survey on Wireless Security: Technical Challenges, Recent Advances, and Future Trends," *Proceedings of the IEEE*, vol. 104, no. 9, pp. 1727–1765, 2016.

[74] A. Mpitziopoulos, D. Gavalas, C. Konstantopoulos, and G. Pantziou, "A survey on jamming attacks and countermeasures in WSNs," *IEEE Communications Surveys Tutorials*, vol. 11, no. 4, pp. 42–56, 2009.

[75] K. Pelechrinis, M. Iliofotou, and S. V. Krishnamurthy, "Denial of service attacks in wireless networks: The case of jammers," *IEEE Communications Surveys and Tutorials*, vol. 13, no. 2, pp. 245–257, 2011.

[76] W. Xu, K. Ma, W. Trappe, and Y. Zhang, "Jamming sensor networks: Attack and defense strategies," *IEEE Network*, vol. 20, no. 3, pp. 41–47, 2006.

[77] W. Xu, W. Trappe, Y. Zhang, and T. Wood, "The feasibility of launching and detecting jamming attacks in wireless networks," *Proceedings of the International Symposium on Mobile Ad Hoc Networking and Computing (MobiHoc)*, pp. 46–57, 2005.

[78] M. Lichtman, R. P. Jover, M. Labib, R. Rao, V. Marojevic, and J. H. Reed, "LTE/LTE-a jamming, spoofing, and sniffing: Threat assessment and mitigation," *IEEE Communications Magazine*, vol. 54, no. 4, pp. 54–61, 2016.

[79] A. S. K. Pathan, H.-W. Lee, and C. S. Hong, "Security in wireless sensor networks: issues and challenges," in *2006 8th International Conference Advanced Communication Technology*, vol. 2, 2006, pp. 6 pp.–1048.

[80] X. Wang, P. Hao, and L. Hanzo, "Physical-layer authentication for wireless security enhancement: Current challenges and future developments," *IEEE Communications Magazine*, vol. 54, no. 6, pp. 152–158, 2016.

[81] OASIS Standard, "MQTT Version 3.1.1." [Online]. Available: http://docs.oasis-open.org/mqtt/mqtt/v3.1.1/os/mqtt-v3.1.1-os.html

[82] "Eclipse Mosquitto™, An open source MQTT broker." [Online]. Available: https://mosquitto.org/

[83] L. Meng, A. Luna, E. R. Díaz, B. Sun, T. Dragicevic, M. Savaghebi, J. C. Vasquez, J. M. Guerrero, M. Graells, and F. Andrade, "Flexible System Integration and Advanced Hierarchical Control Architectures in the Microgrid Research Laboratory of Aalborg University," *IEEE Transactions on Industry Applications*, vol. 52, no. 2, pp. 1736–1749, 2016.

[84] "The Things Network." [Online]. Available: https://www.thethingsnetwork.org/docs/

[85] L. Hernández, C. Baladrón, J. M. Aguiar, L. Calavia, B. Carro, A. Sánchez-Esguevillas, J. Sanjuán, Á. González, and J. Lloret, "Improved short-term load forecasting based on two-stage predictions with artificial neural networks in a microgrid environment," *Energies*, vol. 6, no. 9, pp. 4489–4507, 2013.

[86] L. Wen, K. Zhou, S. Yang, and X. Lu, "Optimal load dispatch of community microgrid with deep learning based solar power and load forecasting," *Energy*, vol. 171, pp. 1053–1065, 2019.

[87] W. Kong, Z. Y. Dong, Y. Jia, D. J. Hill, Y. Xu, and Y. Zhang, "Short-Term Residential Load Forecasting Based on LSTM Recurrent Neural Network," *IEEE Transactions on Smart Grid*, vol. 10, no. 1, pp. 841–851, 2019.

[88] A. Géron, *Hands-on Machine Learning with Sklearn, keras & tensorflow*, 2nd ed.   O'Reilly, 2019, vol. 1.

[89] S. Hochreiter and J. Schmidhuber, "Long Short-Term Memory," *Neural Computation*, vol. 9, no. 8, pp. 1735–1780, 1997.

[90] E. J. Palacios-Garcia, A. Moreno-Muñoz, I. Santiago, I. M. Moreno-Garcia, and M. I. Milanés-Montero, "PV Hosting Capacity Analysis and Enhancement Using High Resolution Stochastic Modeling," *Energies*, vol. 10, no. 10, p. 1488, 2017.

References

Part II

Papers

Paper A

Smart Inverters for Microgrid Applications: A Review

Babak Arbab-Zavar, Emilio J. Palacios-Garcia, Juan C. Vasquez, and Josep M. Guerrero

Paper A.

Paper B

Message Queuing Telemetry Transport Communication Infrastructure for Grid-Connected AC Microgrids Management

Babak Arbab-Zavar, Emilio J. Palacios-Garcia, Juan C. Vasquez, and Josep M. Guerrero

Paper B.

Paper C

LoRa Enabled Smart Inverters for Microgrid Scenarios with Widespread Elements

Babak Arbab-Zavar, Emilio J. Palacios-Garcia, Juan C. Vasquez, and Josep M. Guerrero

Paper C.

Paper D

Reducing Detrimental Communication Failure
Impacts in Microgrids by using Deep Learning
Techniques

Babak Arbab-Zavar, Suleiman M. Sharkh,
Emilio J. Palacios-Garcia, Juan C. Vasquez, and
Josep M. Guerrero